Effect of hyperosmolarity and hypoosmolarity on vascular remodeling : either way is a wrong way

Vincent Fleury, Hany Charara, Richard Luscan, Laurent Schwartz

▶ **To cite this version:**

Vincent Fleury, Hany Charara, Richard Luscan, Laurent Schwartz. Effect of hyperosmolarity and hypoosmolarity on vascular remodeling : either way is a wrong way. 2021. hal-03449963

HAL Id: hal-03449963
https://hal.science/hal-03449963

Preprint submitted on 25 Nov 2021

HAL is a multi-disciplinary open access archive for the deposit and dissemination of scientific research documents, whether they are published or not. The documents may come from teaching and research institutions in France or abroad, or from public or private research centers.

L'archive ouverte pluridisciplinaire **HAL**, est destinée au dépôt et à la diffusion de documents scientifiques de niveau recherche, publiés ou non, émanant des établissements d'enseignement et de recherche français ou étrangers, des laboratoires publics ou privés.

Effect of hyperosmolarity and hypoosmolarity on vascular remodeling : either way is a wrong way.

Vincent Fleury[1], Hany Charara[1], Richard Luscan and Laurent Schwartz[2]

1) Laboratoire Matière et Systèmes Complexes, UMR 7057, Université de Paris, CNRS

10 rue Alice Domont et Léonie Duquet 75006 Paris, France.

2) Assistance Publique des Hôpitaux de Paris, Avenue Victoria 75004 Paris, France.

Abstract: The formation of the vascular architecture is a very active and important area of research. A lot of thrust has been put on the study of the effect of haemodynamics and especially the role of shear stress[1-5] on vascular pattern formation. However, the architecture of blood vessels is also quite sensitive to transmural pressure[6-7]. Transmural pressure itself is dependent on metabolism. The effect of transmural pressure has received less attention. In many pathologies tissue pressure plays a crucial role in vascular patterning. At short time scales tensile or compressive stresses may facilitate or hinder perfusion, and at longer time scales stresses impact vascular remodeling. Here, we report a study of the effect of osmotic shocks on the dynamics of vascular pattern formation. Working with the chicken Chorio Allantoic Membrane[8] and Yolk Sac[9], we evidence that blood vessels are in a state of dynamic homeostasis, and that osmotic shocks, either hypertonic or hypotonic, lead to vascular collapse, by entirely different mechanisms. Hypoosmolarity leads to dilation of the interstitium by water uptake, and hyperosmolarity leads to solvent outflux, tension driven shrinkage and subsequent vascular collapse. In summary, compressive and tensile forces in the tissue are finely balanced to enable a proper vascular patterning, shifting the mechanical state either way, is a wrong way.

Introduction

Branching patterns, and especially vascular systems, are ubiquitous in nature[10]. The role of the vascular system is to bring nutrients and oxygen to the tissue and remove wastes and CO2[11]. With a centralized pumping organ such as the heart, a hierarchical system of pipes is necessary to efficiently distribute the blood from the upper scale down towards the capillaries, and back. During development and throughout life, a proper vascular system is formed by spreading endothelial cells which form a plexus of lumenized capillaries[12-14]; these capillaries remodel under the action of the haemodynamic forces[1,3-5,14]. Transmural pressure and shear stress are known to be the principle actors in the remodeling of the vascular system[5,14]. However, the exchanges of gases, the molecular and ionic trafficking, occur at the

smallest scale, the capillary scale, where tissue is in close proximity to the blood and especially in direct contact with the erythrocytes. Across the vessel wall there exists a very strong concentration gradient of molecules such as fat, sugar, etc. The vessel wall and the tissue actively regulate the fluxes, in conjunction with the flow, while sustaining a complex pattern of osmotic pressures of metabolic origin. While vascular alterations at the larger scales can lead to life-threatening strokes (stenosis, aneurism, infarct), these are by definition brutal. At the capillary scale, the situation is different : slow discrete alterations can progressively alter the capillary beds over very long time scales, essentially reducing the number of capillaries and increasing the hemodynamic resistance, up to terminal morbidity and ischemia. Many pathologies, such as hypertension[15], diabetes[16], obesity[17], etc. lead to such systemic problems in the distal capillary compartment, referred collectively as "angiopathies". These are difficult to study because the architectural problems arise at the small scale, over long period of times. The chicken embryo model is a classical model for the study of generic mechanisms of vascular development, alteration or repair, although the dynamics is much accelerated[8]. The extra embryonic organs, the Yolk Sac and the CAM can be used for biological experimentation. However even in these organs, time-lapse imaging down to the smallest scale remains a challenge. A recently developed imaging system makes it possible to film in time-lapse the evolution of the vascular tree at the smallest scale[18,19]. Here we present a dynamic study of the evolution of blood vessels following exposure to osmotic shocks, hypertonic or hypotonic. These supposedly mimmick the effect of a biochemical, metabolic, imbalance. We used exposure of the CAM to Mannitol as an assay causing hyperosmolarity, because Mannitol is a classical compound used in medicine to fight oedema[20] and we used exposure to low concentration PBS of the YS as an assay causing hypoosmolarity. Dynamic analyses of the transient consequences and of the recovery reveal two completely different mechanisms of ischemia, one in which vessel collapse is caused by an excess in tension which amounts to a centripetal compressive stress on the vessels, and one by interstitial tissue dilation which also causes vascular collapse. The dynamics of collapse and of recovery are contra-intuitive, with several phases, including a transient burst of blood flow during vascular collapse caused by a scaling broken symmetry in the vascular tree. We also show that during recovery, blood vessel strands reopen in a sequence analogous to the phenomenon of mud-cracking or tensorial reopening under tensile stress[21,22].

II. Results.

II.1 Static observations

In a first series of experiments we observe the effect of Mannitol on the development of the vasculature in the CAM. We drop four drops of Mannitol at concentration 2.5% (137.5 mOsm/l), or 5% (275 mOsm/l) or 10% (550 mOsm/l) and observe the resulting morphology of the CAM vascular bed (starting day 10). We choose not to go at higher concentrations, because the effect was already so drastic at 10% that there was little point in provoking even

more deleterious effects. We compared the observed morphology at given time intervals, in particular at T=0h, 24h, 48h, 72h. We also compared the treated areas to similar areas far away serving as internal control, on the same embryo. Whenever possible we compared the morphology at points opposite to the treated spot, across the entire CAM (d ~ 3 to 6 cm). Care must be taken to choose an area at approximately the same distance to the center of the CAM, since there is a developmental gradient from proximal to distal in the normal CAM. All images are in vivo images, without any preparation or staining, obtained by the method described in Ref. 19.

Figure 1 shows the CAM vasculature resolved all the way down to the smallest capillaries, for the Mannitol 10% assay. Fig. 1A shows the typical effect of the Mannitol 10% after 3 hours of incubation. The perfusion has ceased in large areas of tissue which are ischemic. Fig. 1B shows the comparison of the vascular beds prior to the Mannitol assay and after 24 hours, in the treated area (same embryo, same area, different time). We observe a loss of capillary vessels of approx. 30% after 24 hours (the capillary loss was calculated by thresholding the images and extracting the mean vascular occupancy in the image). Fig. 1C shows the comparison between the area exposed to Mannitol 10% and a control area on the same CAM, after 24 hours (same embryo, same time, different area). We observe that although there is a progressive recovery, the capillaries, after 24 hours, still exhibit a mean diameter which is reduced by 42% (the reduction in diameter was measured directly on the image by measuring the cross section at mid-height of 110 capillary strands).

Therefore, small vessels tend to collapse, but if they don't, their diameter decrease. They also tend to meander longitudinally. It is classical that vascular collapse is a non-linear buckling process with a threshold, therefore vessel may have a limiting vascular diameter prior to collapse brutaly ; we found a lower cut-off in the treated samples of 6,3μm. Fig. 2A shows the effect caused by exposure to 2.5%, 5% or 10% Mannitol. We clearly see a dose dependent effect, with the 2.5% solution giving a quite modest effect, and the 10% Mannitol giving a very strong effect with transiently complete ischemia (total eclipse of the vessels) in large patches of tissue.

One important static observation is that there exists a capillary gradient in the normal tissue, with capillary loops being smaller along arteries (Fig. 2B). Collapse is more visible on the venous side, such that during an osmotic shock the apparent gradient of capillary loops increases, with voids being larger along the venous bed (see for example Fig. 1A bottom or Fig.1C bottom), up to the point that large ischemic areas are formed. This suggests that the tissue stress drives vascular collapse. However, it also suggests that in the normal instance, tissue stress already regulates a capillary gradient. It is generally assumed that the capillary bed is uniform, our observations show that it is not.

Also, we observe that in a given area, the apparent ischemia associated to the capillary collapse tends to occur first at the branching point.

II.2 Dynamics of the osmotic shock.

We followed by Time-Lapse the evolution of the vascular bed as a function of time. The effects are of course more dramatic at a concentration of 10%. We observe a rapid collapse of the vascular bed, with a pattern of tissue contraction (Fig. 3A to the right, from Video 1, shows the displacement map extracted by Particle Imaging Velocimetry (PIV) : a contraction of the tissue is observed). More quantitatively (Fig. 3B) we can follow the vascular density during the collapse. This evidences a slow passive collapse, followed by a more rapid collapse showing an active contraction of the tissue, confirming the visual impression of Video 1 (Fig. 3B).

It is natural to expect a massive collapse of the vessels to stop the perfusion. However, contrary to intuition, a remarkable and unexpected phenomenon was observed. During the active phase of the vascular collapse, the vascular tree tends to collapse in an orderly fashion, with larger arterioles collapsing more strongly than the smaller ones. This induces an unexpected phenomenon: there exists a residual flow during the collapse which pushes deterministically the stagnant blood from the larger scale down towards the capillaries (Fig.4). This is particularly spectacular in accelerated time-lapse imaging (Video 2) which shows a flash of blood being flushed down into the capillary plexus by the end of the collapse, while the collapsed arterioles are transiently reopened and reperfused. This observation implies that during the active collapse of an arteriolar bed, and even in the absence of connection to the heart, there exists *wired in* the tree architecture a spontaneous tendency to push the flow in the physiological direction, by means of a broken scaling symmetry –large branches contract more than small branches, the contraction implies an increased tension T, which creates an excess pressure ΔP by Laplace's law $T/R=\Delta P$, and a flux by Poiseuille's law $V=-(R^2/12\mu)\text{grad}(P)$, in which R is the radius and μ the viscosity.

II.3 Dynamics of recovery

In this experimental assay, although the blood vessels may be completely collapsed at places, the tissue is still properly oxygenated since it receives oxygen supply directly from atop and not only from the vascular flow. Therefore, the vascular bed is in a state of ischemia with respect to metabolic wastes, but not with respect to oxygen (no actual hypoxia). This is why the assay does not induce any visible necrosis. This allows us to follow the progressive recovery of the perfusion.

Fig. 5A Shows the evolution of one area exposed to mannitol 10%, at T0+24hrs, T0+48hrs, T0+72hrs. We observe that the tissue progressively recovers. However, there exists non uniform areas in which reperfusion is retarded (arrows). We notice that these areas correspond to the vicinity of the veins, and that there exists a gradient of perfusion during recovery, with capillaries and vessels being more collapsed on the venous side.

In order to understand the mechanism of recovery in more detail, we followed by time-lapse the recovery. Contrary to intuition, the collapsed ischemic area does not recover by a

progressive percolation of the flow across a collapsed capillary plexus. Much to the contrary, we observe that vessels tend to reopen suddenly, by opening across wide areas by a single strand, as if an entire domain was split by a new capillary path (Fig. 5B and Video 3). Generally, the reopening of perfusion across a wide domain tends to occur perpendicularly to the main axis of the domain, in a way akin to Hertwig's law for cell division[23], or Douady and Couder's law for leaf venation[21].

In Fig. 5B, we observe that at several scales, the capillary strands would reopen following grossly the segmentation of the domain across the shortest path perpendicularly to the longest axis of the void. When subsequent reopenings would occur (Fig. 5B bottom), they tend to occur at right angles, such that a wide domain is first split by a capillary strand in two smaller domains, which next tend themselves to be split in even smaller domains by strands which tend to be orthogonal to the previous splitting event at the upper scale. This process is reminiscent of material (mud, china etc.) cracking under tensile or compressive stress[21]. It is known that tensile cracking is a scale-invariant fractal-like process. Similarly, here, the relief of the compressive stress tends to reopen progressively the entire plexus in a hierarchical fashion, albeit influenced by the existing noisy network pattern (the "cracks" have to follow existing strands).

II. 4 Hypotonic shocks of the Yolk Sac.

In the CAM assay with Mannitol, we clearly observe a vascular collapse due in part to reduction of tissue volume by an osmotic outflow of water (the tissue dries off in an attempt to dilute the Mannitol). We wished to observe the opposite effect, in an osmotic shock also. This is why we turned to the chicken Yolk-Sac (YS). The chicken YS is another extra-embryonic organ, which is in contact with the yolk. Its developmental role is to digest the yolk with enzymes, store glycogen, deliver cholesterol to the circulation, produce enzymes, etc.[24]. In short, it serves as nourishment organ for the embryo. It is a classical observation that the YS has multiple villosities underneath which increase the surface for nutrient uptake. It is known that the YS is full of fat and glycogen[24]. This is why the YS is not as transparent as the CAM. We expected that exposing the YS to a simple solution of PBS would provoke an osmotic shock related to the mismatch in osmolarity between the PBS and the cytosol of YS cells. Since the very purpose of the YS is to transfer molecules from the yolk to the vasculature, it forcibly is porous to some extent.

We therefore observed the embryo in a dual set up by which the embryo is observed recto-verso, one microscope filming the vasculature from atop, and a second one from underneath. The set-up for such a dual acquisition was presented in Ref. 25. This generates such data as Fig. 6A, and Video 4 in which, for the sake of clarity, the image of the villosities has undergone a mirror symmetry so that its orientation is the same as the direct image of the vessels.

We indeed observed following exposure to a concentrated 1/2X PBS solution (Dulbbeco), that the Yolk Sac tissue would swell, and blood vessels would collapse (Fig 6A). The dual imaging allows one to observe simultaneously the dilation of the villosities (Fig. 6A Right, Video 5), and how they tend to compress the vessels, thus participating in vascular collapse (Fig. 6A Left). High resolution of the villosities dilation (10X) shows villosities dilation and vascular compression at cell resolution level (Video 5), revealing a scaling mechanism by which scaling compressions compress vessels in a hierarchical pattern (Fig. 6B).

Much surprisingly, a residual vessel flow which empties larger vessels and flushes the stagnant blood towards capillaries downscale is also observed in this assay. Another observation is that the area which lines up the arteries and is normally at the boundary between the lumen, and the villosities, swells, and appears very conspicuously as a swollen ribbon along the arterioles (Fig.7A, arrows). Simple inspection of the YS shows indeed that in the normal YS, there already exists an area in which capillary density is reduced. The comparison of the normal endoderm, and the endoderm exposed to the osmotic shocks (Fig. 7C) confirms that the dilation of the endoderm lining the vessels goes up to confluence thus crushing the capillaries in between.

II. Discussion

The osmotic assays reveal several facts. First of all, both the hypertonic and hypotonic assay lead to ischemia, which was not *a priori* intuitive. In the first case, ischemia is due to passive (simple tissue dryness) and active myogenic contractions of the tissue and the vessels within, which both contribute to crush the vascular lumens. While in the second case, the ischemia is due to interstitial tissue swell which pumps up water and swells, so that the vessels within the tissue are crushed. The result is qualitatively the same: collapse of the vascular bed and interruption of perfusion. This shows that the blood vessels are in a state of homeostasis, bounded on one side by tissue compressive stress, and from the other side by tissue and vessel tensile stress. If tissue compressive stress is increased, the tissue dilates and the vessels are squeezed, if tissue and vascular tension is increased, the entire tissue shrinks, and the vessels are also squeezed. That water outflow causes tissue contraction is understandable in that it increases saline concentration. Actin-myosin contraction is well known to be dependent on Calcium concentration[26]. In order to check that the CAM was indeed contractile in the first place, we performed simple electric shocks, following the set up described in Ref. 27. We indeed found that short electric shocks (5 seconds), of moderate tension (0.1 to 0.5V) would in 100% of the cases cause a rapid contraction of the CAM (by minutes) much similar to the one observed in the Mannitol assay, both in intensity and in time scale (Fig. 8A, Video 6). This shows that the CAM has a contractile behavior, and that contraction does induce vascular collapse and ischemia on a typical time scale of minutes. We also checked by staining for α-Actin, that the CAM contains contractile muscle-like cells (Fig. 8B), we found that Actin was present around the mature vessels (arrow), and also along a thin layer alongside the ectoderm (arrowhead). We thus conclude that the entire CAM can

constrict, with a stronger active tension around vessels, that this constriction can be stimulated by a change in polarity, but equally by an osmotic imbalance causing water traffic.

Secondly, we find that the hierarchical structure of the branching structure leads to a dynamic broken symmetry which favors flow downstream. This suggests that arteriole contraction may contribute to normal flow albeit modestly. That circulation may happen in the absence of heartbeat is a hypothesis which has been raised by several physiologists[28,29], suggesting the possibility that vascular tone could contribute to flow. The finding that contraction of the arteriolar tree provokes, in this assay, a residual flow, raises the possibility that arteriolar flow may exist in the absence of a heartbeat. This view is coherent with the mechanism of flow in primitive taxa such as myxomicetes ("the blob" Ref. 30) and in lymphatics[31], and it would not be surprising that circulation by distributed contraction along the arterial tree might have preceded active flow by a centralized pump such as a heart. This is, to some extent, what is observed in the cephalochordate *Amphioxus*[32]. On physical grounds, a structural broken symmetry implies a dynamic broken symmetry, which may pump fluid in the lumen. In this view, it makes sense that arteries have more pericytes and muscle cells than veins, so that there is no retrograde flow.

We also reveal a mechanism of recovery by which thin capillary strands reopen in a hierarchical manner, following the existing collapsed plexus. Although the plexus represents a rather noisy lattice, the strands tend to reopen and be reperfused in a pattern of perpendicular, tensorial, long ranged, scaling order, as observed in leaf venation[21], and more generally in stress release cracks such as drying mud or china cracking. This shows that reperfusion after ischemia is controlled by tissue stress and not by blood flow. This is to say that, in the absence of perfusion, the reopening does not follow any haemodynamic cue (it can't since there is no flow), but follows the sequence of stress relief across a stressed domain, with stress relief propagating information at long range. This observation fits also with evolutionary issues or concepts, in that it makes sense that such a scaling process should be favored, as it allows the tissue to recover at the gross scale faster than a progressive loop by loop percolation. In mud or china cracking, the crack occurs when the tensile stress exceeds a threshold with a criterium for cracking such as the von Mises' criterium[33]. Here the situation is different in that the vessels are collapsed and the relief of the compressive stress will reopen the vessel when the criterium for vascular collapse (pipe buckling) is reached. However, in both cases the criterium for opening corresponds to a physical threshold (buckling threshold, or cracking threshold).

With respect to pathological situations, the CAM assay presented here is reminiscent of what is observed in typical œdema, either caused by metabolic problems, thrombosis, cancer progress, etc. The Yolk Sac assay is also reminiscent of what is observed in angiopathies in which capillary regression is observed, by which capillaries disappear in excess along arterioles. This process is observed physiologically[7] and it is important to

generate a functional vascular tree. Already in a functional vasculature, a capillary gradient is apparent between veins and arteries. This capillary gradient, in the case presented here, is related to a metabolic stress gradient from the arteries towards the veins (see also Ref. 7 for in vivo measurements of tissue compliance between arteries and veins by air puff tonometry). However, whenever the stress is too high, capillaries are crushed, which causes an excess of capillary reduction. Then, the tissue is ill perfused, and a mechanism which is useful during development and vascular remodeling, becomes detrimental. We suggest that Virchow-Robin spaces and lacunae[34] observed along arterioles in the brain, and which can cause brain seizures may also be related to the phenomenon described here.

The dynamic observation of vascular remodeling during such simple osmotic shocks reveals a wealth of dynamic biomechanical features, especially at the very small scale, which are often overlooked. Often, the spatial resolution is too coarse, or in vivo time-lapse studies are not possible. Addressing the dynamics of angiopathies requires both an adapted temporal resolution and a fine spatial resolution, as can be achieved in the CAM model.

We should also mention that in 2 out of 20 CAM experiments we observed the formation of aberrant anastomoses and varicose vessels, never observed in the normal CAM (Supplementary Material Figure 1). Considering the low frequency of this event we were not able to study it in more detail, however shunt or fistula formation is in practice a medical issue in vascular pathologies[35].

Hyperosmolarity is a frequent feature[36,37] in diseases such as inflammation and cancer. In both set of diseases, there is extensive vascular remodeling. One of the hallmarks of cancer is sustained angiogenesis[38,39]. Next, the vasculature around the tumors remodel abnormally, forming multiple arterio-venous shunts and ischemic areas. Hyperosmolarity in itself is known to induce neoangiogenesis[40]. The transcription and the secretion of VEGF is enhanced by osmotic pressure[41,42]. We did not address in this work specifically the impact of an osmotic shock on endothelial cells proliferation, since our imaging system allows one to follow perfused vessels only. While we hypothesized that metabolic shifts induce hyperosmolarity, reciprocally hyperosmolarity can induce metabolic shifts, as shown recently[43]. Our results should help to sort out the different phenomena at play during pathological neoangiogenesis and remodeling.

.

References

1 Mulvany, M. J., Baumbach, G. L., Aalkjaer C., Heagerty A.M., Korsgaard N., Schiffrin E. L., Heistad D. D. Vascular remodeling. *Hypertension* **28**, 505–506 (1996).

2 Price, R. J., Less, J. R., Van Gieson, E. J., Skalak T. C. Hemodynamic stresses and structural remodeling of anastomosing arteriolar networks: design principles of collateral arterioles. *Microcirculation* **9**, 111-124 (2002).

3 Fleury, V. & Schwartz, L. DLA from shear stress as a simple model of vasculogenesis. *Fractals* **7** (1), 33-39 (1999).

4 Zakrzewicz, A., Secomb, T. W., Pries, A. R., Angioadaptation: keeping the vascular system in shape. *News Physiol Sci* **17**, 197–201 (2002).

5 Pries, A.R., Reglin, B., Secomb, T.W. Remodeling of Blood Vessels Responses of Diameter and Wall Thickness to Hemodynamic and Metabolic Stimuli. *Hypertension* **46** (4), 725-731 (2005).

6 Secomb, T.W., Dewhirst, M.W., Pries A. R. Structural Adaptation of Normal and Tumour Vascular Networks. *BCPT* **110**, 63-69 (2012).

7 Al-Kilani, A., Cornelissen, A., T.-H. Nguyen, T.-H., Lorthois, S., Lenoble, F., Unbekandt, M., Fleury, V. During vertebrate development arteries exert a morphological control over veins through physical factors. *Phys Rev E* **77**, 051912 (2008).

8 Ribatti D. Chick embryo chorioallantoic membrane as a useful tool to study angiogenesis. *Int Re Cell Mol Biol* **270**, 181-224 (2008). doi: 10.1016/S1937-6448(08)01405-6. PMID: 19081537.

9 Le Noble, F., Moyon, D., Pardanaud, L., Yuan, L., Djonov, V., Mattheijssen, R., Bréant, C., Fleury, V., Eichmann, A. Flow regulates arterio-venous differentiation in the chick embryo yolk-sac. *Development* **131**, 361-375 (2004).

10 Fleury V., Leonetti M. and Gouyet J.-F. *Branching in nature,* Springer Verlag/EDP Sciences (2001).

11 Jarvis, S**.** Vascular system 1: anatomy and physiology. *Nursing Times* **114** 4, 40-44 (2018).

12 Gerhardt, H., Golding, M., Fruttiger, M., Ruhrberg, C., Lundkvist, A., Abramsson, A., Jeltsch, M., Mitchell, C., Alitalo, K., Shima, D., & Betsholtz, C. VEGF guides angiogenic sprouting utilizing endothelial tip cell filopodia. *The Journal of cell biology* **161** (6), 1163–1177 (2003). https://doi.org/10.1083/jcb.200302047

13 Davis, G. E., Stratman, A. N., Sacharidou, A., Koh, W. Molecular basis for endothelial lumen formation and tubulogenesis during vasculogenesis and angiogenic sprouting. *Int Rev Cell Mol Biol* **288**, 101-65 (2011). doi: 10.1016/B978-0-12-386041-5.00003-0. PMID: 21482411; PMCID: PMC3891664.

14 Campinho, P., Vilfan, A., Vermot, J. Blood Flow Forces in Shaping the Vascular System: A Focus on Endothelial Cell Behavior. *Frontiers in Physiology* **11**, 552 (2020). URL=https://www.frontiersin.org/article/10.3389/fphys.2020.00552 DOI=10.3389/fphys.2020.00552

15 Li Y., Ishikawa, H., Matsuyama, H., Shindo, A., Matsuura, K., Yoshimaru, K., Satoh, M., Taniguchi, A., Matsuda, K., Umino, M., Maeda, M., Tomimoto, H. Hypertensive Arteriopathy and Cerebral Amyloid Angiopathy in Patients with Cognitive Decline and Mixed Cerebral Microbleeds. *J Alzheimers Dis* **78** (4), 1765-1774 (2020). doi: 10.3233/JAD-200992. PMID: 33185609.

16 Xu, L., Kanasaki, K., Kitada, M., Koya, D. Diabetic angiopathy and angiogenic defects. Fibrogenesis. *Tissue Repair* **1 5** (1), 13 (2012) doi: 10.1186/1755-1536-5-13. PMID: 22853690; PMCID: PMC3465576.

17 Bouissou, H., Pieraggi M. T., Julian M., Flores, R. Micro-angiopathy and the dermal connective tissue in obesity. *Annales D'Anatomie Pathologique* **22** (2), 117-32, (1977).

18 Fleury, V. Device for imaging blood vessels, EPO patent N° 18305795.9-1132 22/06/2018

19 Richard, S., Brun, A., Tedesco, A., Gallois, B., Taghi, N., Dantan, P., Seguin, J., Fleury, V., Direct imaging of capillaries reveals the mechanism of arteriovenous interlacing in the chick chorioallantoic membrane. *Commun Biol* **1**, 235 (2018).

20 Tenny, S., Patel, R., Thorell, W. Mannitol. In: StatPearls [Internet]. Treasure Island (FL): StatPearls Publishing (2021).https://www.ncbi.nlm.nih.gov/books/NBK470392/

21 Couder, Y., Pauchard, L., Allain, C., Adda-Beddia M. & Douady, S. The leaf venation as formed in a tensorial field. *Eur. Phys. J. B* **28**, 135–138 (2002). https://doi.org/10.1140/epjb/e2002-00211-1

22 Laguna, M. F, Bohn, S., Jagla, E.A. The Role of Elastic Stresses on Leaf Venation Morphogenesis. *PLoS Comput Biol* **4** (4), (2008): e1000055. https://doi.org/10.1371/journal.pcbi.1000055

23 Hertwig, O., (1884). Das Problem der Befruchtung und der Isotropie des Eies. Eine Theorie der Vererbung. *Jenaische Zeitschrift für Naturwissenschaft* **18**, 274 (1884).

24 Wong, E. A, Uni, Z. Centennial Review: The chicken yolk sac is a multifunctional organ. *Poult Sci* **100** (3), 100821 (2021). doi:10.1016/j.psj.2020.11.004

25 Fleury, V. Clarifying tetrapod embryogenesis by a dorso-ventral analysis of the tissue flows during early stages of chicken development. *Biosystems*, *Special issue "Morphogenesis"* **109**, 460, (2012).

26 Kuo, I.Y., Ehrlich, B.E. Signaling in muscle contraction. *Cold Spring Harb Perspect Biol* **7** (2) (2015). :a006023. Published 2015 Feb 2. doi:10.1101/cshperspect.a006023.

27 Fleury, V. & Murukutla, A. Electrical stimulation of developmental forces reveals the mechanism of limb formation in vertebrate embryos. *EPJE* **42**, 104 (2019).

28 Alexander,W. Branko Furst's Radical Alternative: Is the Heart Moved by the Blood, Rather Than Vice Versa? *P T* **42** (1), 33-39 (2017).

29 Manteuffel-Szoege, L., Michalowski, J., Grundman, J., Pacocha, W. On the possibility of blood circulation continuing after stopping the heart. *J Cardiovasc Surg (Torino)* **7** (3), 201–208 (1966).

30 Yamada, H., & Nakagaki, T. Flow Rate Driven by Peristaltic Movement in Plasmodial Tube of Physarum Polycephalum. *AIP Conference proceedings* **1028** (1), 210 (2008) 10.1063/1.2965090.

31 Gashev, A. A. Physiologic aspects of lymphatic contractile function: current perspectives. *Ann N Y Acad Sci.* **979**, 178-87 (2002). doi: 10.1111/j.1749-6632.2002.tb04878.x. PMID: 12543727.

32 Moller, P. C. & Philpott, Ch. W. The circulatory system of *Amphioxus* (*Branchiostoma floridae*). *J Morph* **139**, 39406 (1973).

33 Barthélémy J.-F., Dormieux L., Kondo D. Determination of the macroscopic behaviour of a medium with frictional cracks. *C R Acad Sci Mécanique* **331**, 77-84 (2003).

34 Heier, L.A., Bauer, C.J., Schwartz, L., Zimmerman, R.D., Morgello, S., Deck, M.D.F. Large Virchow-Robin spaces: MR-Clinical correlation. *AJNR* **10**, 929 (1989).

35 Barhum, L., What is an arterio-venous fistula?, *Verywell health*, May 2018. https://www.verywellhealth.com/arteriovenous-fistula-5116891

36 Schwartz, L., Guais, A., Pooya, M., & Abolhassani, M. Is inflammation a consequence of extracellular hyperosmolarity? *Journal of inflammation* **6** (1), 1-10 (2009).

37 Schwartz, L., Coldwell, D. Is Liver Disease Caused by Increased Pressure? Interstitial Pressure as a Causative Mechanism in Carcinogenesis and in the Differential Blood Supply in Liver Tumors from the Hepatic Artery. *J Liver* **3** (3), 156-159 (2014).

38 Welter, M., Bartha, K., & Rieger, H. Emergent vascular network inhomogeneities and resulting blood flow patterns in a growing tumor. *Journal of theoretical biology* **250** (2), 257-280 (2008).

39 Hanahan, D., Weinberg, R. A. The hallmarks of cancer. *Cell* **100** (1), 57-70 (2000).

40 Madonna, R., Montebello, E., Geng, Y. J., & De Caterina, R. High glucose promotes angiogenesis by induction of COX-2 and MMP in human endothelial cells via hyperosmolarity changes involving aquaporin-1 and Na/H exchanger-1. *Cardiovascular Res Supp*,**87** (S125) (2010)

41 Hollborn, M., Vogler, S., Reichenbach, A., Wiedemann, P., Bringmann, A., & Kohen, L. Regulation of the hyperosmotic induction of aquaporin 5 and VEGF in retinal pigment epithelial cells: involvement of NFAT5. *Mol Vis* **21**, 360-377 (2015).

42 Veltmann, M., Hollborn, M., Reichenbach, A., Wiedemann, P., Kohen, L., & Bringmann, A. Osmotic induction of angiogenic growth factor expression in human retinal pigment epithelial cells. *PLoS One* **11** (1), e0147312 (2016).

43 Hamraz, M., Abolhassani, R., Andriamihaja, M., Ransy, C., Lenoir, V., Schwartz, L., Bouillaud, F. Hypertonic external medium represses cellular respiration and promotes Warburg/Crabtree effect. *The FASEB Journal* **34** (1), 222-236 (2020).

Ethics statement : All experiments performed in this work are authorized under french law R214-87 on animal experimentation, which permits justified scientific experimentation on embryonic forms of oviparians.

Authors contribution statement. Vincent Fleury, Richard Luscan and Laurent Schwartz designed the experiments and participated in the writing of the manuscript. The experiments were carried out by Vincent Fleury. Hany Charara (undergraduate student) participated in the experiments and especially, did the α-actin stainings in the CAM.

Acknowledgement. Vincent Fleury acknowledges the support and help of Nicolas Chevalier.

Supplementary Material Methods

Chicken CAMs

Shell less culture of embryos is a classical procedure, often used for cancer graft studies[8]. Eggs are cracked before 96 hours and the content is tranferred to a plastic cup. The plastic cup is put inside a Falcon Petri dish 150mmx25mm. PBS (Dubbelco, purchased by Avantor) is poured around the cup in the Petri dish, to provide moisture. The boxes are placed in a custom incubator Thermo Fischer at 37°C. The boxes are carefully opened under a hood once per day to vent the box.

Time-Lapse imaging

Time-lapse acquisition is done with a Basler monochrome CMOS 1920x1200 pxls camera interfaced by ImageJ and purchased by Phase gmbh. Images are registered with the *StackReg* module. Particle Imaging Velocimetry is used to extract the pattern of movement, using the *Tracker* module developped by Olivier Cardoso and Bérangère Abou. The software is available upon reasonable request.

The high resolutions capillary networks are extracted with a patented software[16] which was described in a previous publication[17]. The software is available upon reasonable request.

Osmotic shocks

Osmotic schoks are given by exposing the CAM to a solution of Mannitol in 1X PBS. The Petri dish in which the embryo is incubated is opened, and drops of Mannitol are deposited with a 2ml PPE transfer pipette. The YS is exposed to PBS concentration 0.5X by dipping the YS in the solution of PBS. Yolk Sacs are prepared by cutting a circle around the YS and trasferring the YS with a spoon to a Petri dish where the yolk is carefully rinsed away with a pipette, prior to imaging the YS with a dual system. This dual imaging system comprises a Leica binocular on one side and an Optem tube-lens on the other side. The two magnifying apartus each carry a camera, hooked to a system of data acquisiton. Images are assembled by ImageJ (from Wayne Rasband, at NIH). Standard Mannitol and PBS are purchased from VWR-Avantor.

Electric shocks

Electric shocks are given with 2 thin (50μm) copper electrodes wired to a Hewlett-Packard pulse generator. The electrodes are approached with a Newport translational stage controlled in X and Y with a stepper motor, and by hand in Z with a precision labolift. The potential drop between electrodes was fixed between 0.1 and 0.5 V. The polarity was maintained for 5 seconds.

Actin staining in the CAM.

CAM pieces are fixed in PFA 4% for one hour, then left in saccharose 40% overnight. The samples were embedded in OCT and frozen (-80°C), then cut in a cryo microtome (slice thickness 14μm). The samples were stained with a primary anti-α-Smooth Muscle -1 antibody, from Merck, which is specific of the single isoform of α-smooth-muscle Actin. Samples are dipped in a solution of PBS+triton (0.1%) and BSA containing the antibody, overnight. The samples are then rinsed in PBS, and a secondary antibody is applied (Rabbit Cy3) by leaving the samples one hour dipped in the slution of Cy3. In toto samples were dipped in the Cy3 solution for 3 hours.

Dual observation

For the dual observation of yolk-sac recto verso, the eggs are cracked in a plastic cup before the end of the 4th day. The YS is cut off from the vitelline membrane with fine scizzors. The YS is transferred to a Petri dish with a spoon. The YS is rinsed carefully in PBS with a 2ml PPE Pasteur transfer pipetete. Then the YS is put on a custom stand having a window underneath and one on top. An Optem tube is used to observe the YS from atop and a Leica binocular MZLF III is used to observe the YS from underneath. Two cameras are mounted one on each optical path. The images are mounted in ImageJ (from NIH, author Wayne Rasband). Light is shone with a 1600W lamp from Leica.

Supplementary Material Videos

Video 1 Time-Lapse Video of the contraction observed when the CAM is exposed to Mannitol 10% (Cropped from a Time-Lapse at Mag. 3X, duration 50 Minutes).

Video 2 Time-Lapse video of the contraction of the CAM during exposure to Mannitol 10% showing a final flush of blood downstream from arterioles towards the capillary bed. (Mag. 4X, duration 1 Hour).

Video 3 Time-Lapse video of recovery of the vascular bed after exposure to Mannitol 10% (Cropped from a Time-Lapse at Mag. 3X, duration 9h)

Video 4 Dual Time-Lapse video of the Yolk Sac as filmed from atop and underneath with two optical systems. Exposure to low contration PBS leads to tissue swell by water uptake, and vascular collapse (Mag. 2X, duration 90 Minutes).

Video 5 High resolution Time-Lapse (Mag. 10X) of endodermal cells dilation during exposure to low contration PBS. The endoderm lining the vessels dilate in an orderly fashion, with a final confluence of the dilated zones causing the collapse of the smaller vessels (duration 20 Minutes).

Video 6 Example of CAM contraction following a short (5 Sec.) electric shock of magnitude 0.1V. The CAM constricts in a temporal and spatial pattern similar to the one observed with Mannitol. (Cropped from a Time-Lapse at Mag. 6X, duration 5 Minutes)

Figures and captions

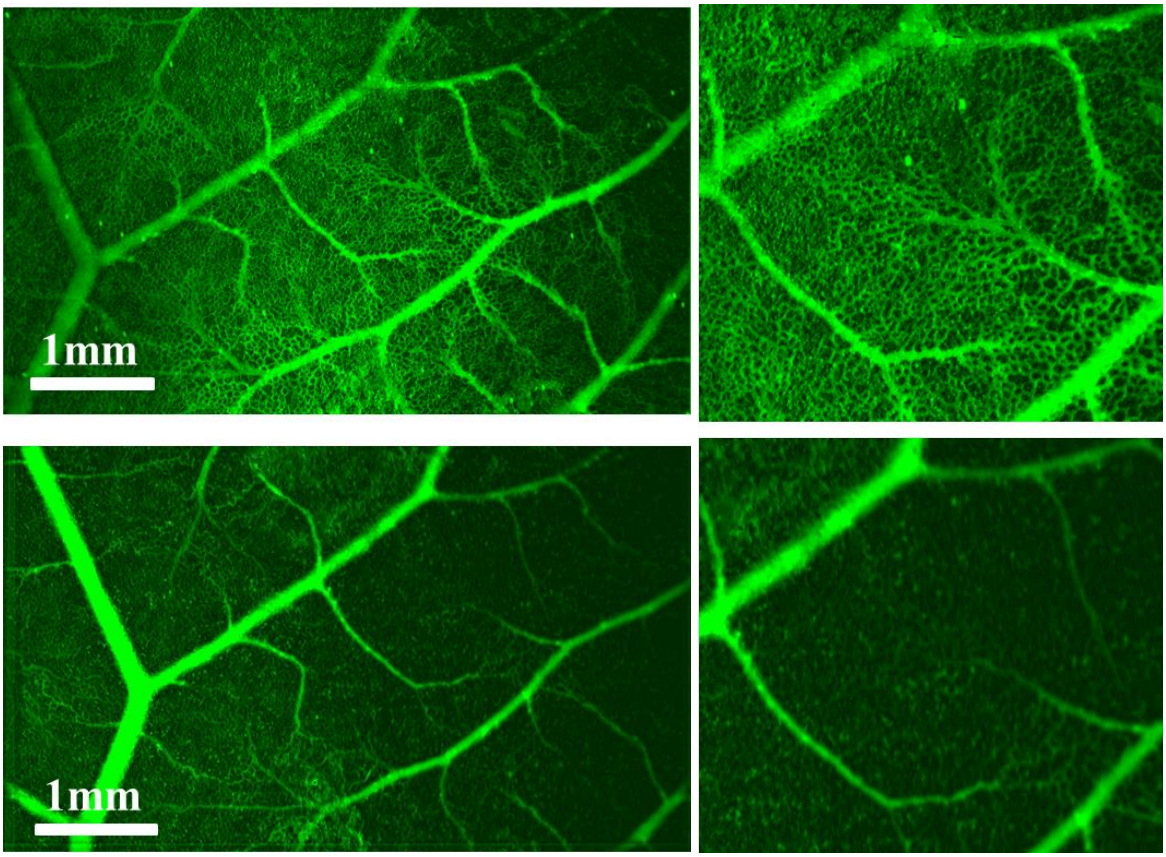

Figure 1A

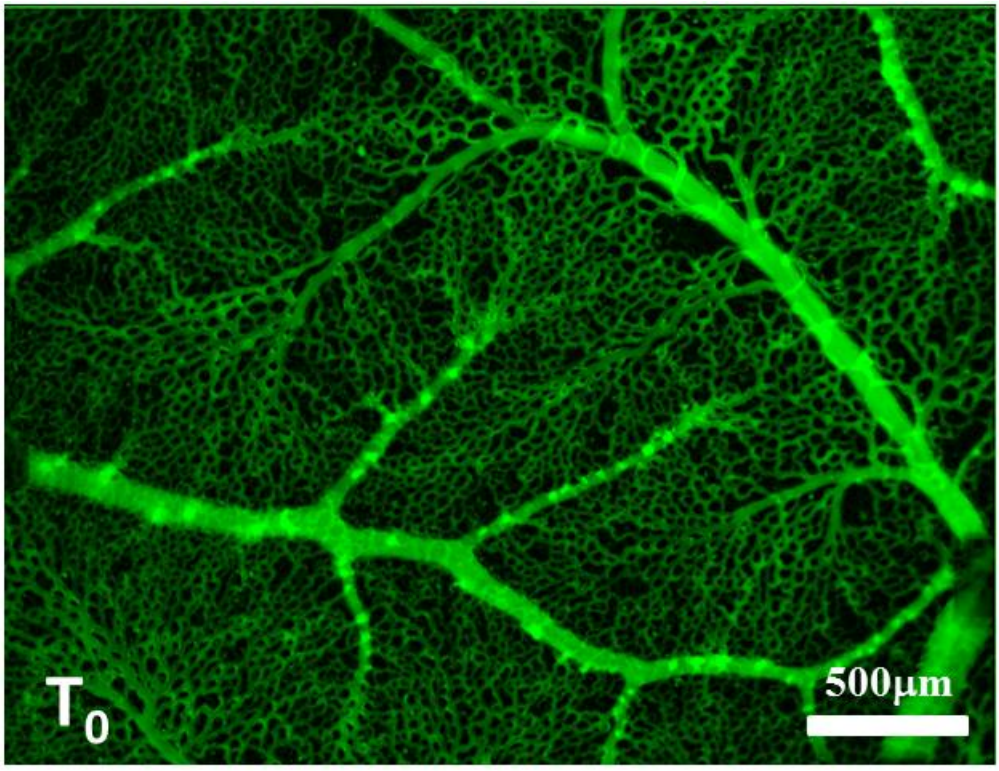

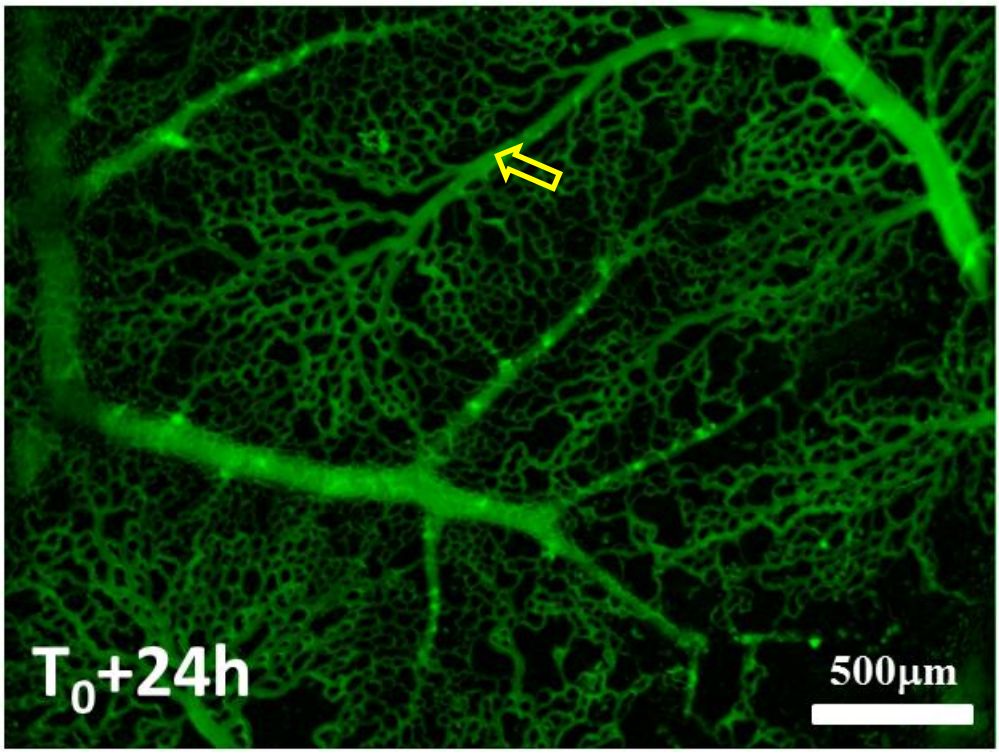

Figure 1B

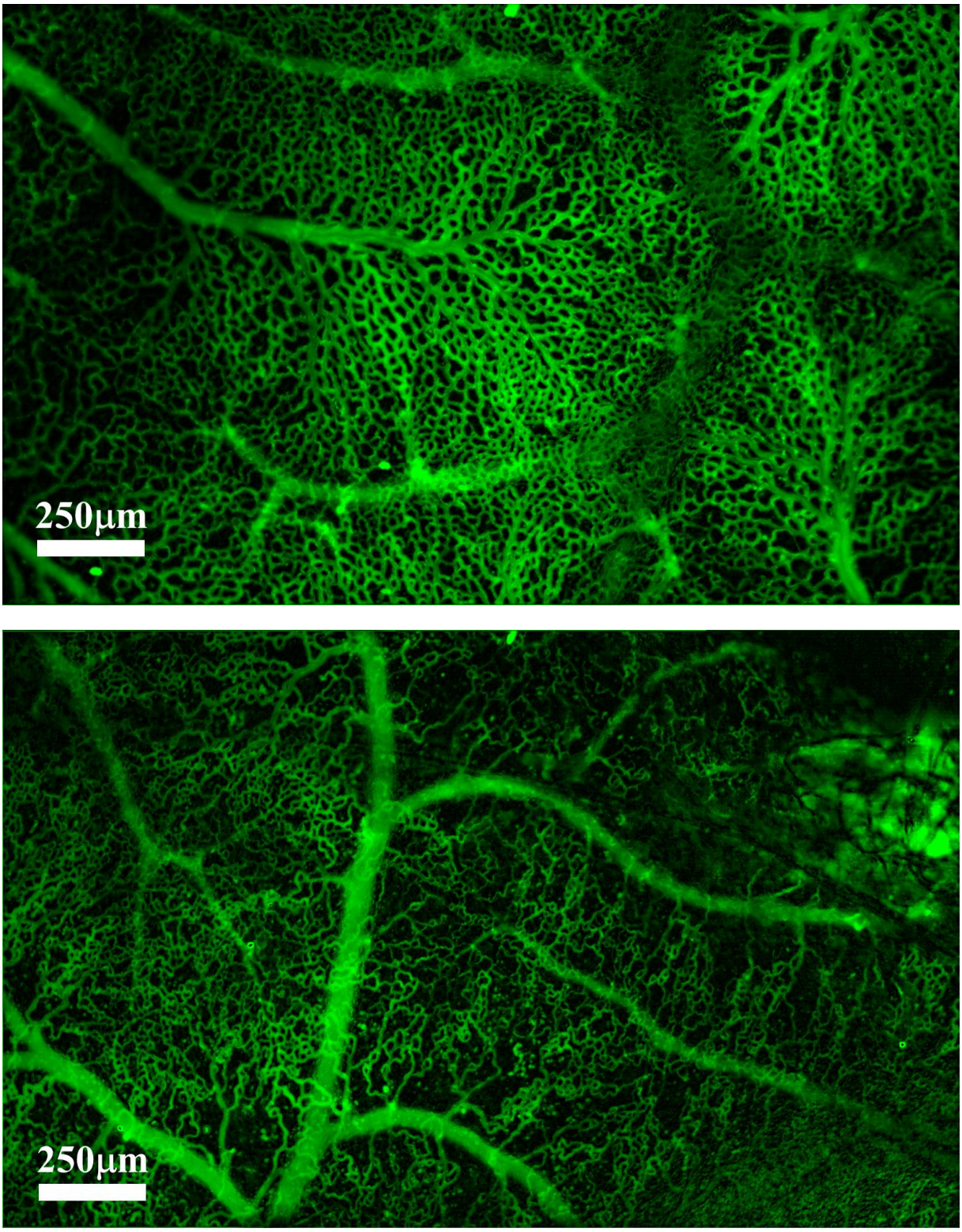

Figure 1C

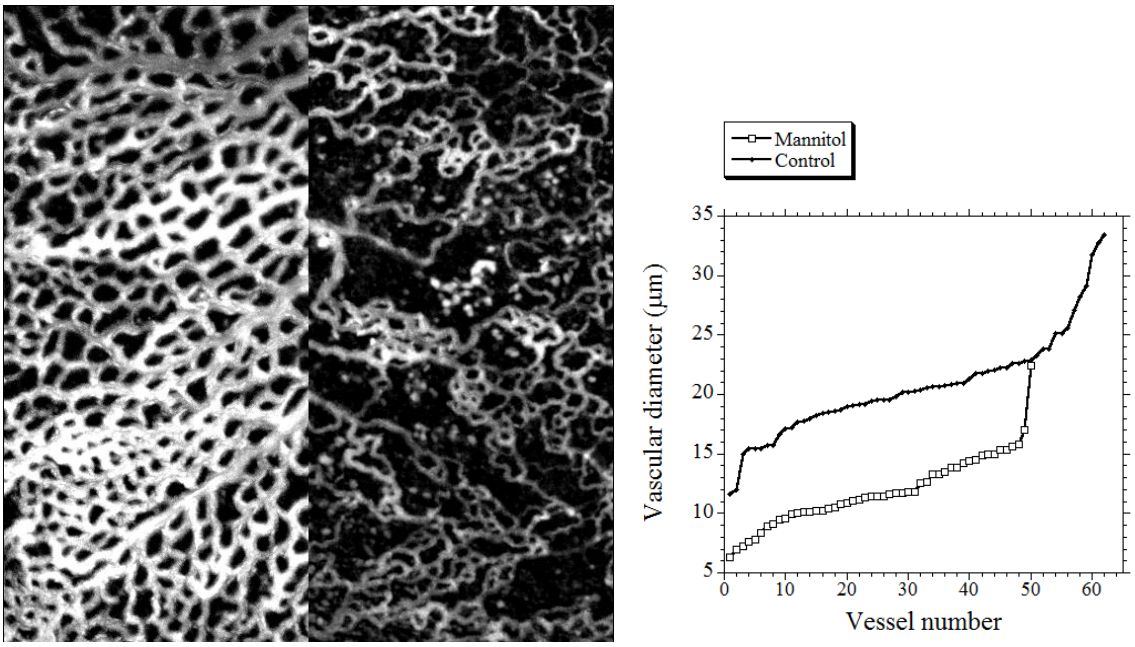

Figure 1D

Figure 1. Effect of Mannitol 10% on the development of the CAM vasculature. Fig. 1A The CAM Vascular bed prior to the Mannitol assay and 3 hours after droping 4 drops of Mannitol 10%. Fig. 1B Comparison of a vascular bed at start of the Mannitol assay (J10) and 24 hrs after exposure to Mannitol 10% (same embryo, same area). Fig 1C Comparison of the area exposed to Mannitol and the control area at a distance of approx. 5 cms, 24 hours after exposure to 10% Mannitol (same embryo, different area). The lacunarity was measured by thresholding and measuring the density of the vascular pattern in the image. It was found that the lacunarity increases by 30% (approximately one third of the vessels are lost after 24hrs**). Fig. 1D** Sample of images used to determine the variation in vascular diameter; to the left the control, to the right the Mannitol-treated area, at T= 24 hours. In this assay, the variation in diameter, excluding the value "0", is in average 42% down (if a capillary is not collapsed, its diameter is in average 42% smaller than the normal capillary). The cutoff for capillaries collapse is found to be 6,3 micrometers.

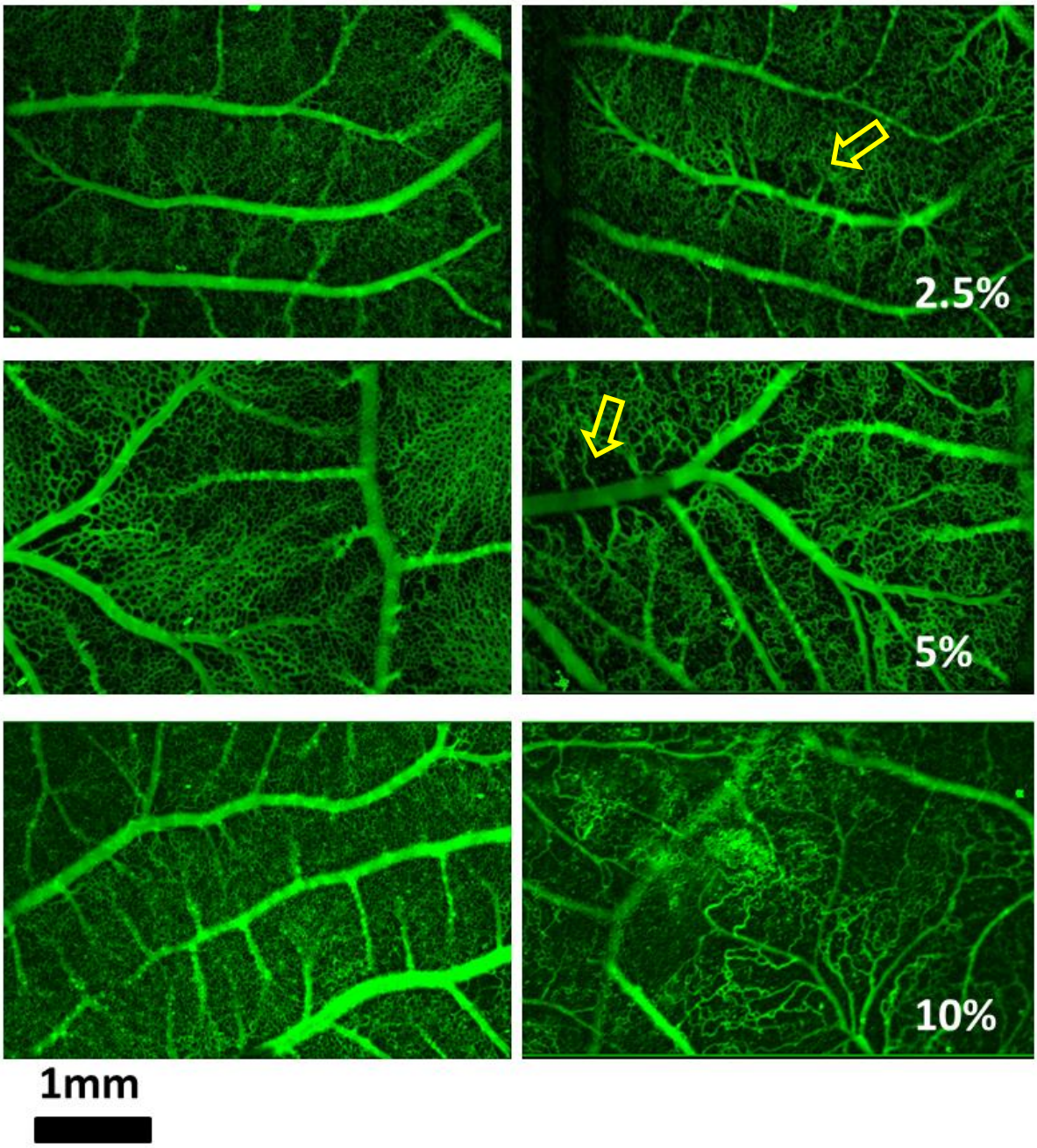

Figure 2A

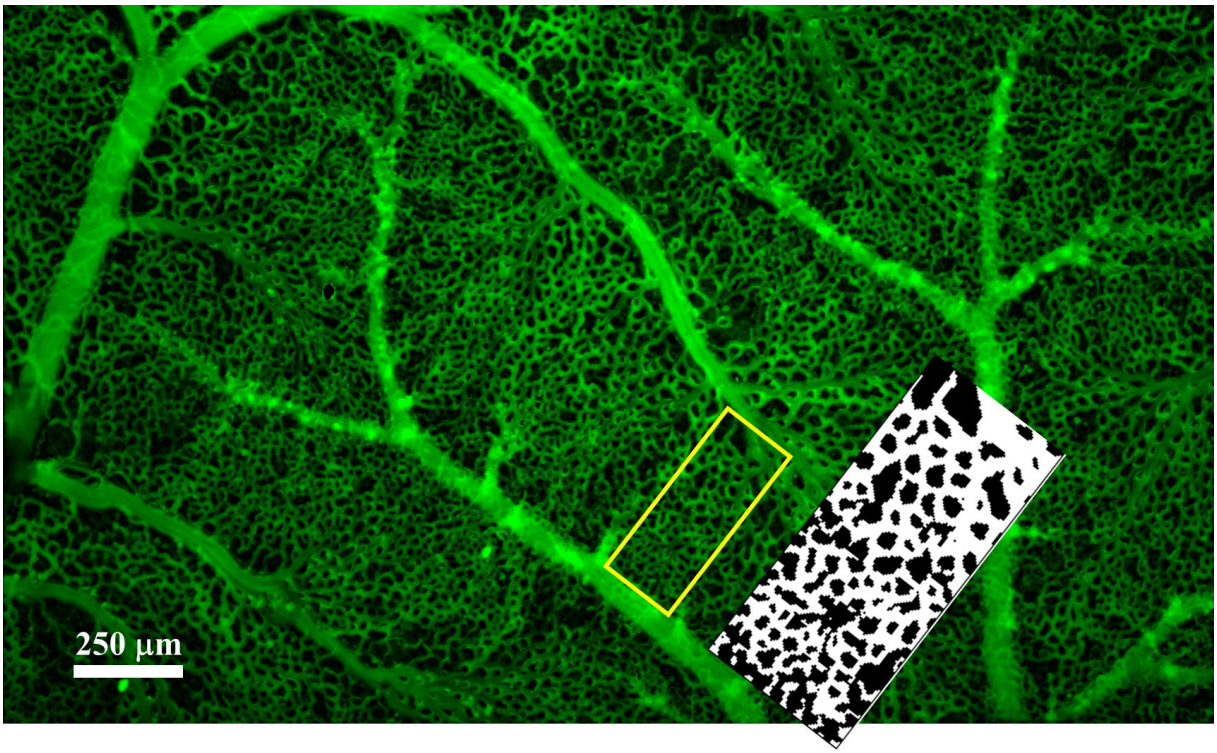

Figure 2B

Figure 2 Fig. 2A. Comparison of the effet of the osmotic shock for 3 concentrations of the Mannitol 2.5% , 5% and 10 %, 4h after the exposure to the Mannitol. There is a dose dependent effect, with the Mannitol at 2.5% giving only a modest effect. The effect is initially more apparent along venules, where voids or lacunae devoid of capillaries form (arrows). Fig. 2B**.** The normal CAM presents a gradient of capillary loops of the order of 60% (the ratio of the capillary loop diameter along the artery over along the veins is 1.6, as deduced from images such as this one, by thresholding, and extracting the mean loop size). The Mannitol assay shows an increase in capillary loop gradient up to 5X as visible for example in Fig. 1A, bottom: the arrow points to 3 capillary lacunae along the venule, perfused by 15 capillary loops along the neighboring arteriole

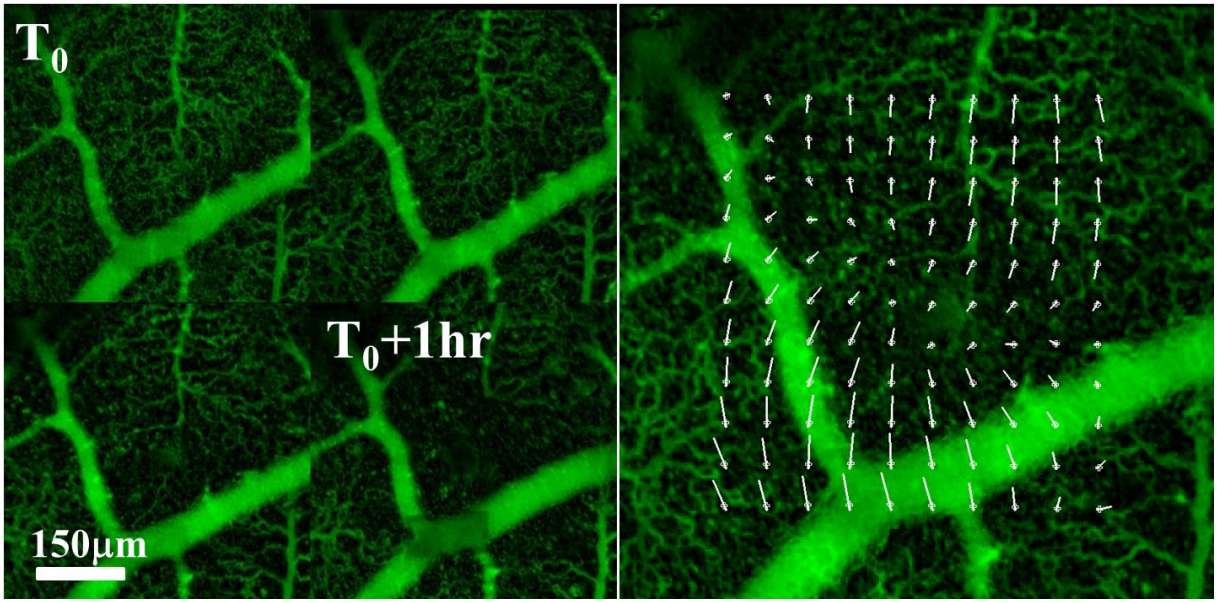

Figure 3A

Figure **3B**

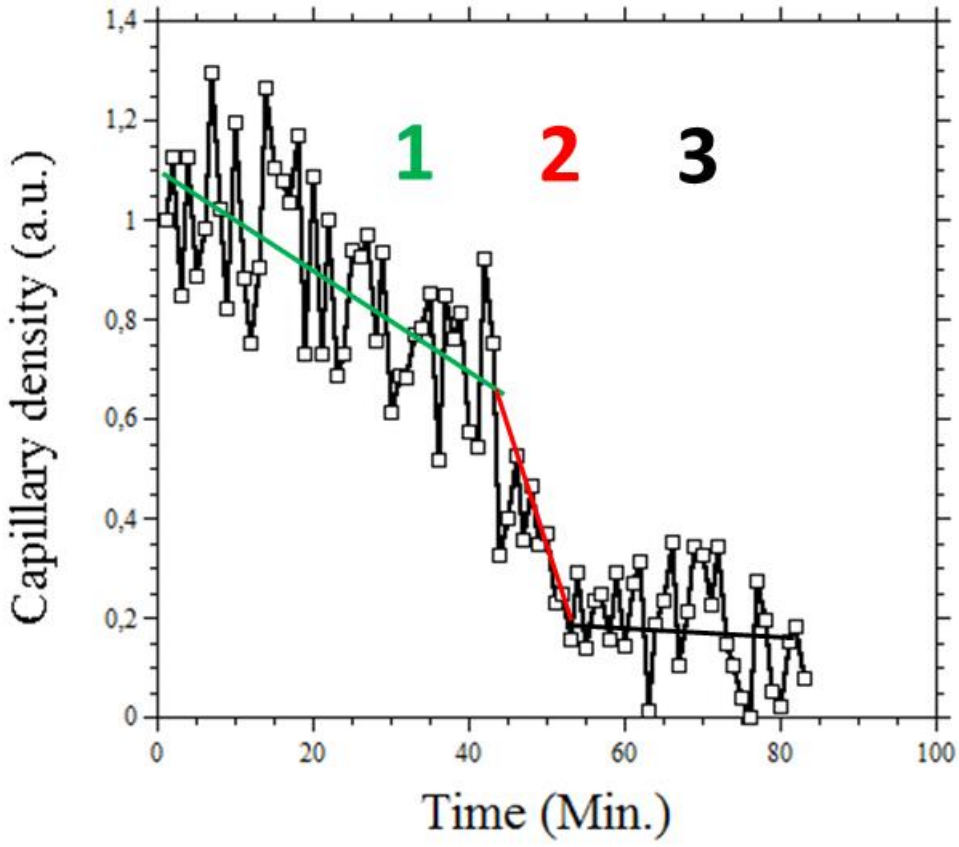

Figure 3. Dynamics of the vascular collapse. Fig. 3A Evolution of the capillary density (from Video 1). Qualitatively, the ischemia occurs by a slow contration of the capillary bed. The movement can be determined by Particle Imaging Velocimetry (Fig. 3A Right) which confirms a contraction pattern during the vascular collapse. Fig. 3B Quantitative analysis shows one first slow phase during which capillary collapse commences, then a second more rapid collapse, and a final ischemic steady state. The noise corresponds to actual oscillations of the tissue.

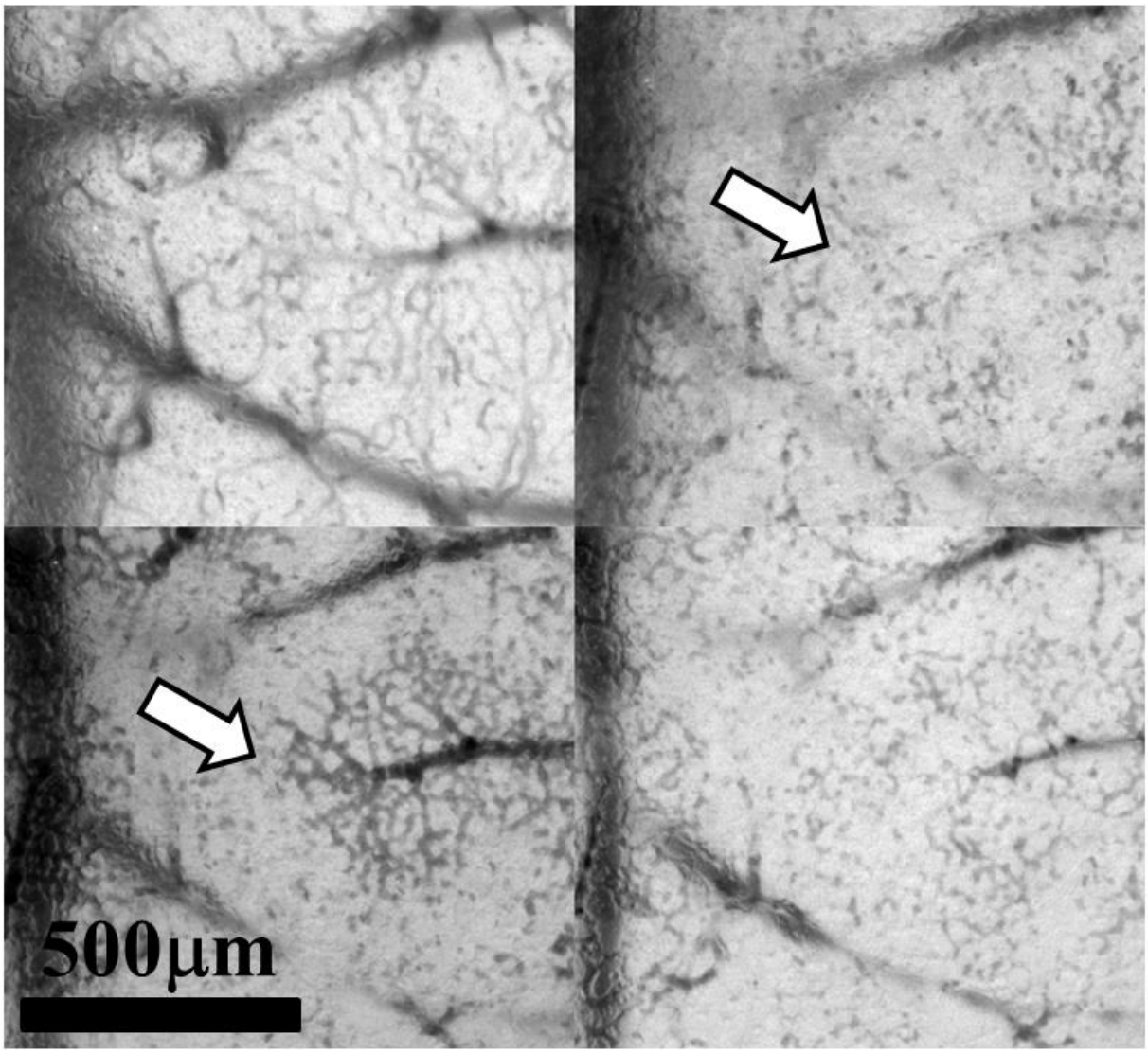

Figure 4

Figure 4. Residual flow during final stages of vascular collapse. During the initial phase of the osmotic shock, the vasculature collapses (Top Left to Top Right). The arrow points to a fully ischemic area. In the next minutes, a small residual flow appears such that distal arterioles transiently reopen and the capillary bed is briefly reperfused (Bottom Left). All snapshots from Video 2. The origin of this phenomenon lies in the hierarchical nature of the vascular

collapse. As vessel collapse proceeeds, collapse occurs first in the distal capillaries. However, the larger vessels collapse later, but more strongly, and they are able to push the flow in a proximal to distal direction towards the already ischemic areas, since vessel contraction creates a fluid pressure (by Laplace's law) pushing the fluid by Poiseuille's law, thus transiently reopening arterioles and capillaries (See Video 2).

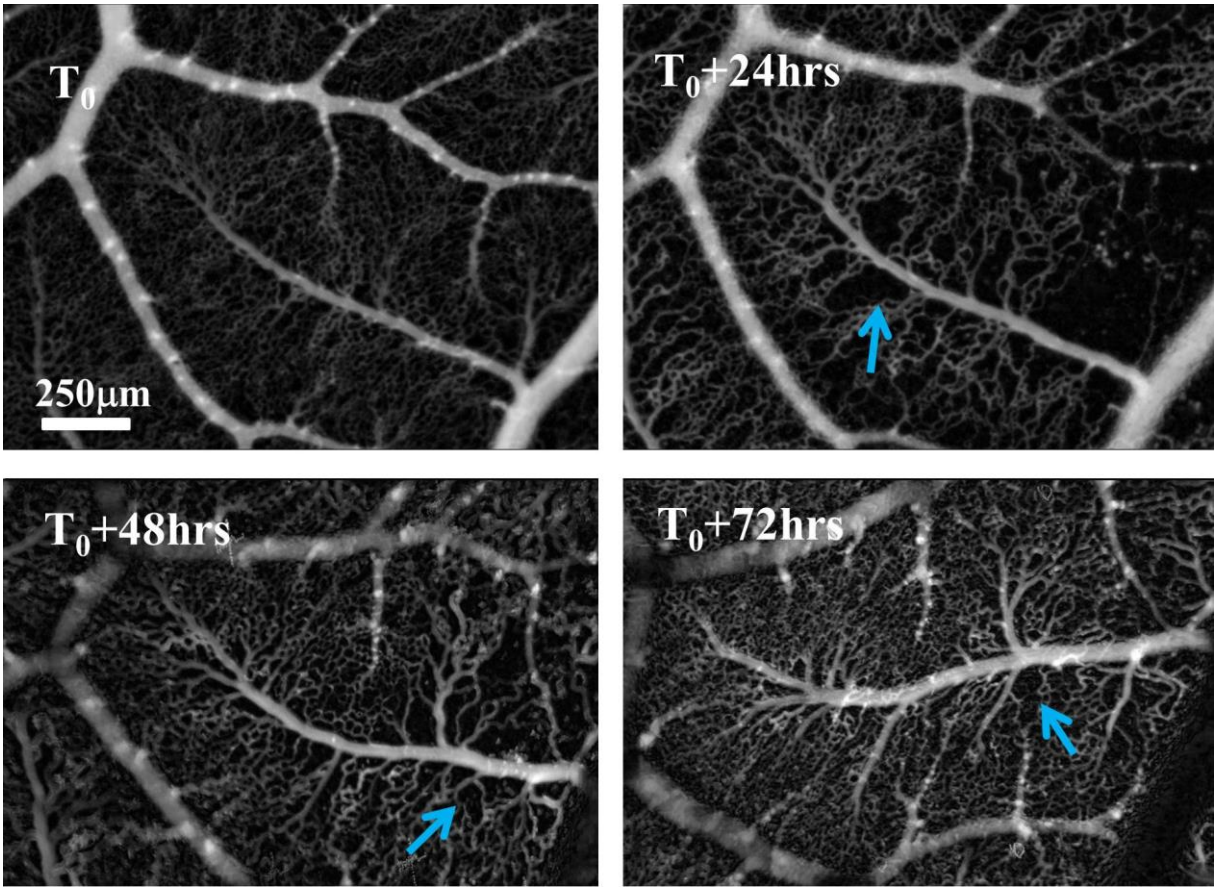

Figure 5A

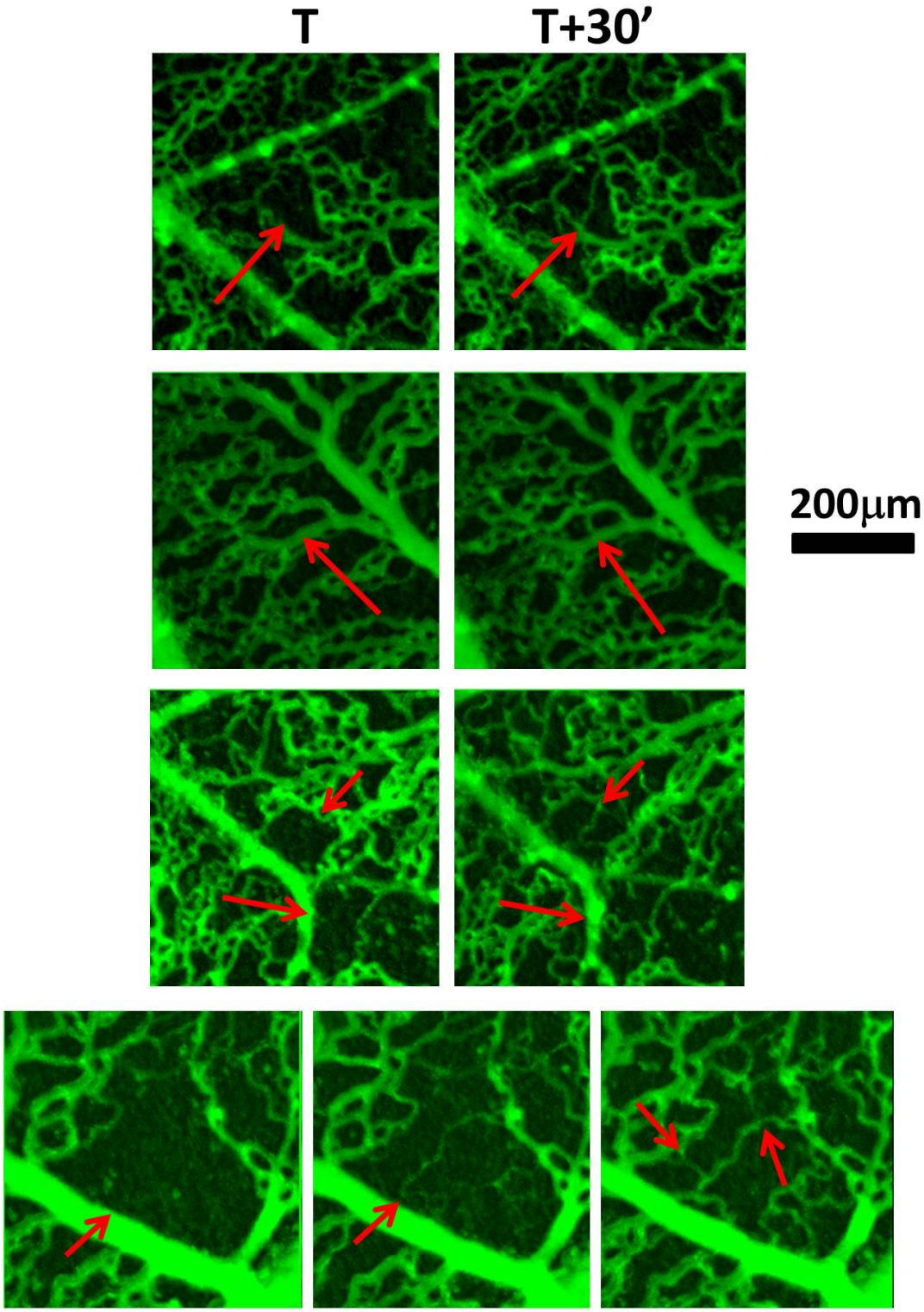

Figure 5B

Figure 5. Dynamics of reperfusion. Fig. 5A Evolution of an area exposed to Mannitol 10%, over 72 hours. It is observed that the already existing gradient of capillary density between venules and arterioles increases steeply, with voids of dryness appearing closer to the venous side (blue arrows). While vascular remodelling proceeds, the venous side is retarded by the absence of flow. Quantitative analysis of the capillary density shows an increase of capillary density of 60% from veins to arteries in the normal vascular bed (Top-Left) and an increase of capillary density, after 24hrs, of about 500% from the collapsed area (venous side) towards the arteriolar side. Fig. 5B Detailed analysis of reperfusion of the ischemic areas. Reperfusion occurs progressively, with small capillary strands reopening following paths that cross dark dry areas, which tend to be perpendicular to the longer axis (arrows). Subsequent openings (bottom, from Left to Right) show that the second reopening tends to be perpendicular to the first. Carefull observation of the Video 1 shows that during the vascular collapse a similar phenomenon actually occurs in the reverse order.

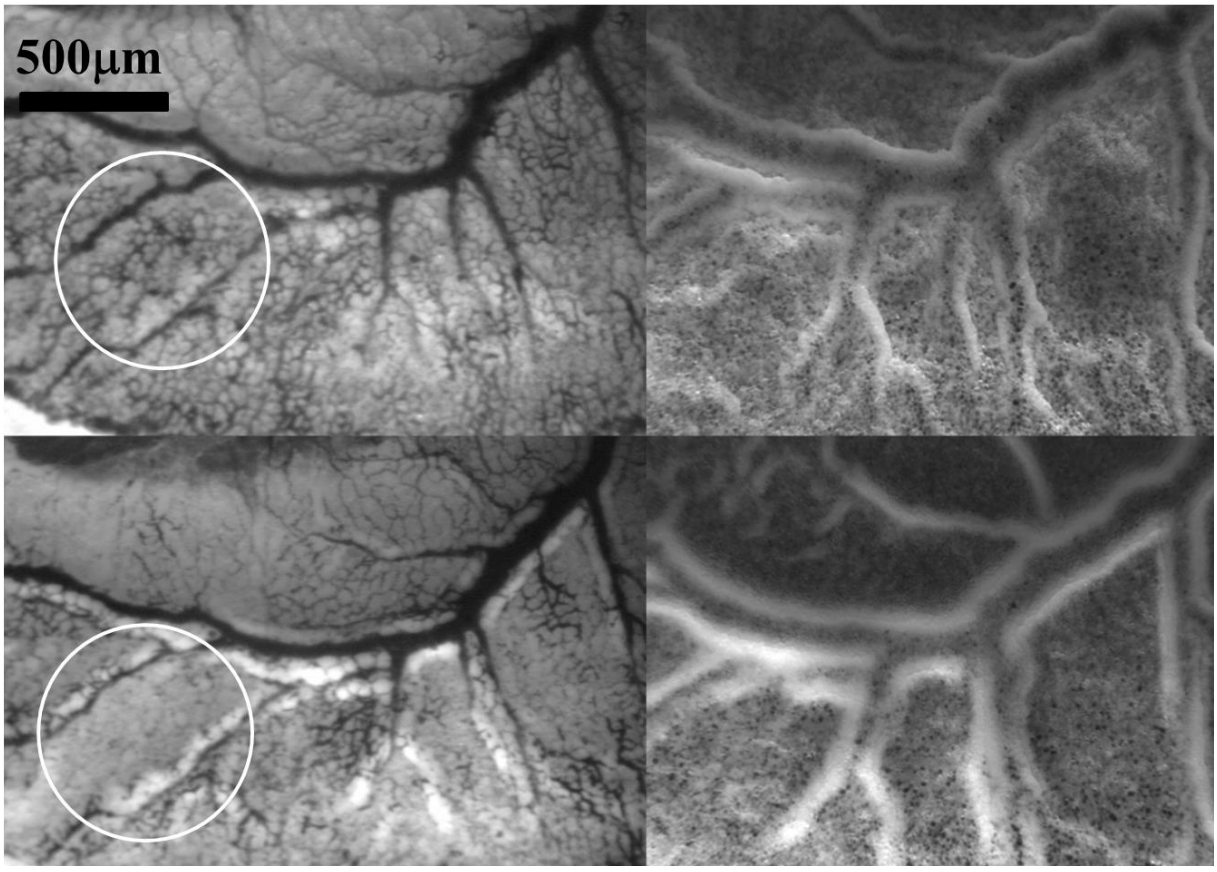

Figure 6A

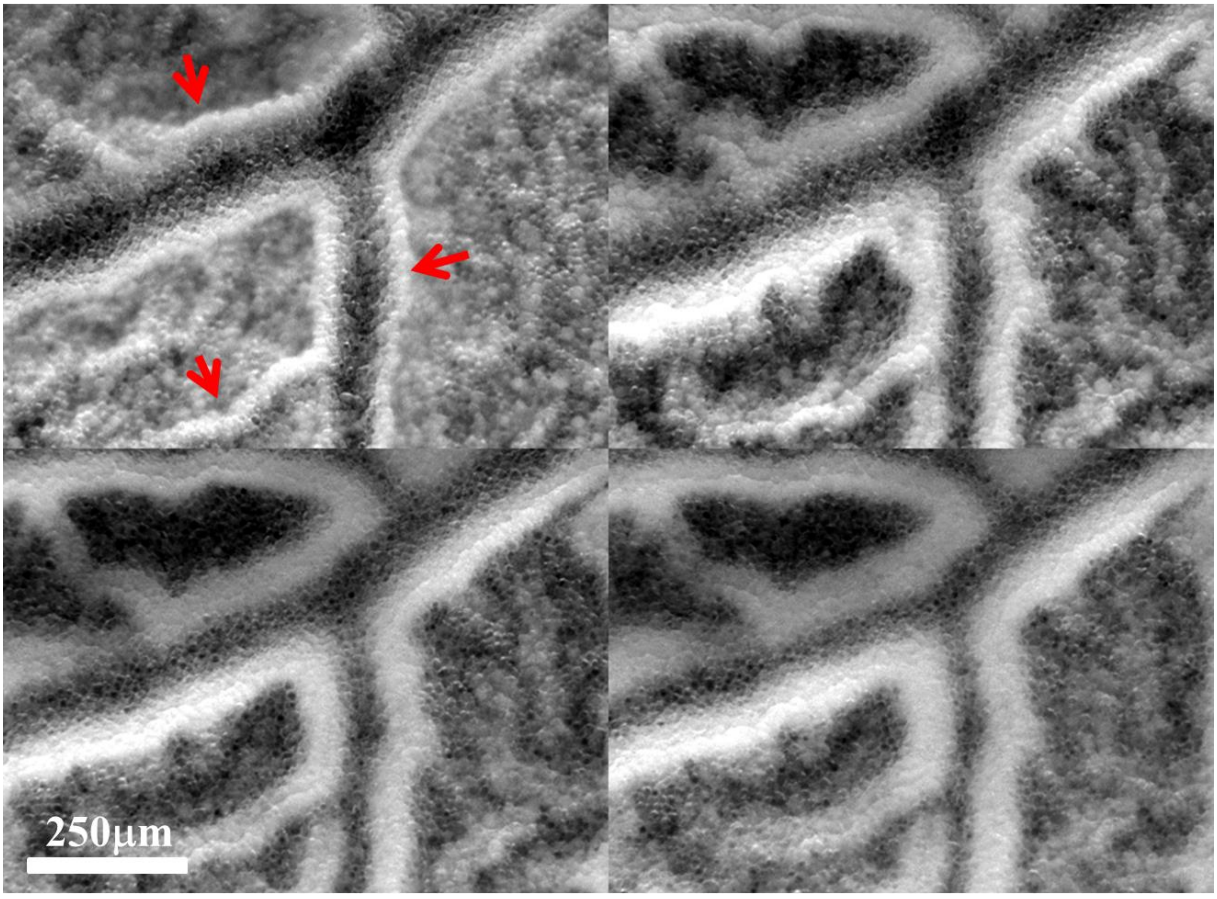

Figure 6B

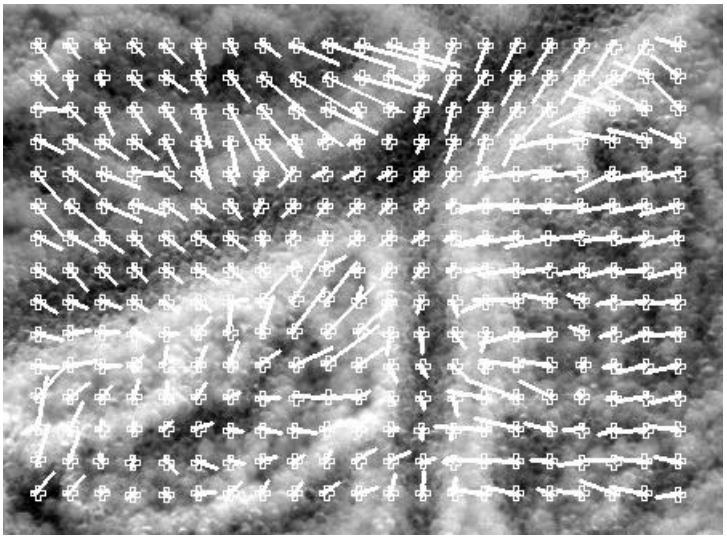

Figure 6C

Figure 6 Effect of a hypotonic shock. Fig. 6A The Yok Sac (day 5) is exposed to PBS at a concentration 0.5X. A dual imaging in Time-Lapse is performed in which both the top layer and the underneath layer are simultaneously imaged. One observes a dilation of the tissue, which progressively crushes the capillaries, as seen from atop, large patchs of tissue devoid of perfused capillaries appear (ischemia, see Video 4). The large circle shows one ischemic

area. Underneath, the endoderm lining the vessels swells (Video 4). Fig. 6B Detailed Time-Lapse imaging of the endoderm shows a scaling dilation of the endoderm lining the vessels (see Video 5). The red arrows point to three levels of arterioles in the hierarchy. Fig. 6C Extraction of the displacement map by Particle Imaging Velocimetry shows a dilation of the interstitium (the movements expand in the interstium) and that the movement crushes the vessels (the dilations of several domains collide against each other along a vessel, see Video 5).

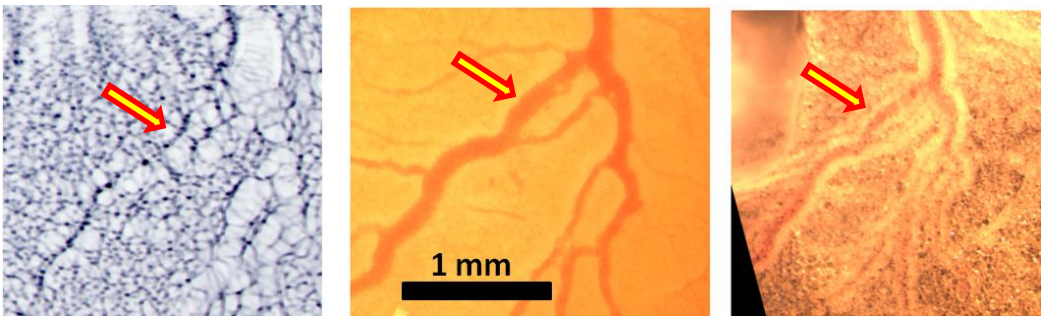

Figure 7A

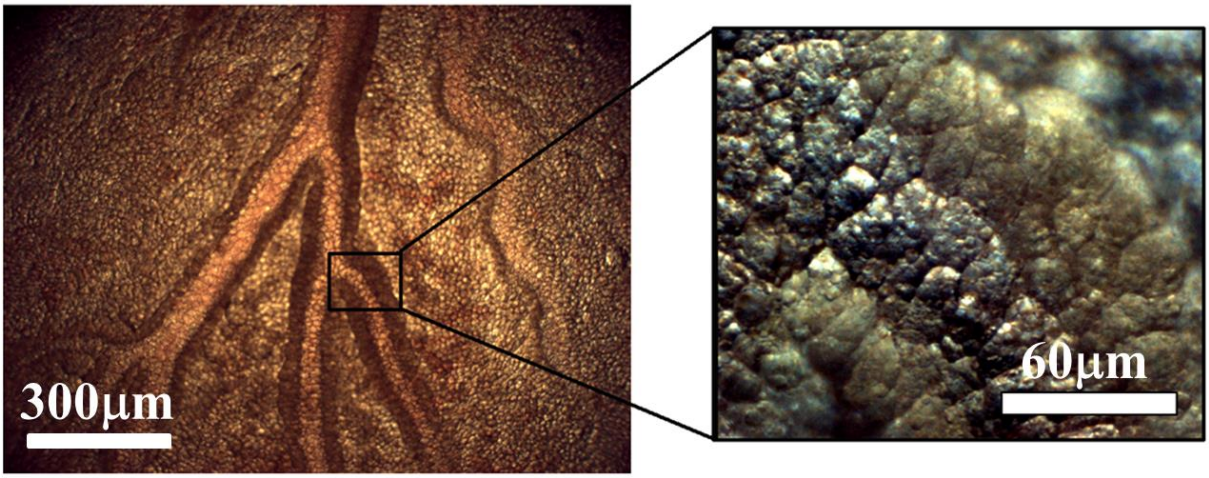

Figure 7B

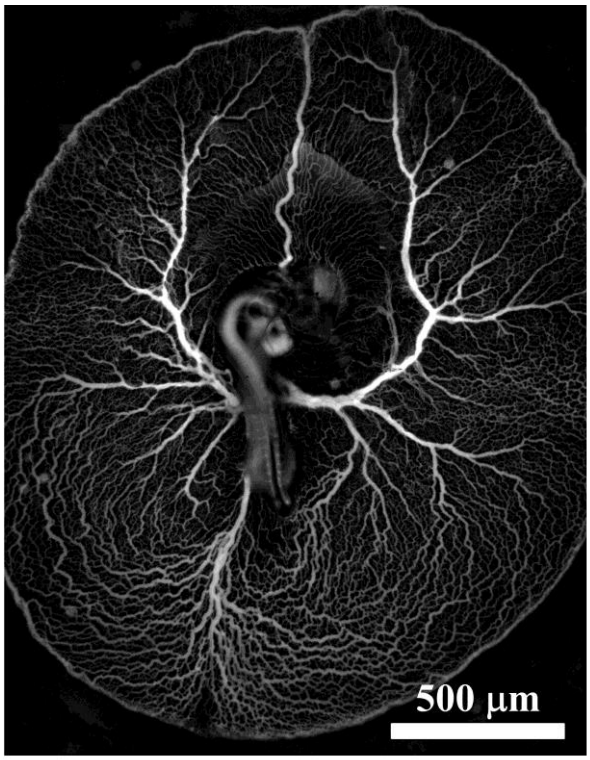
500 μm

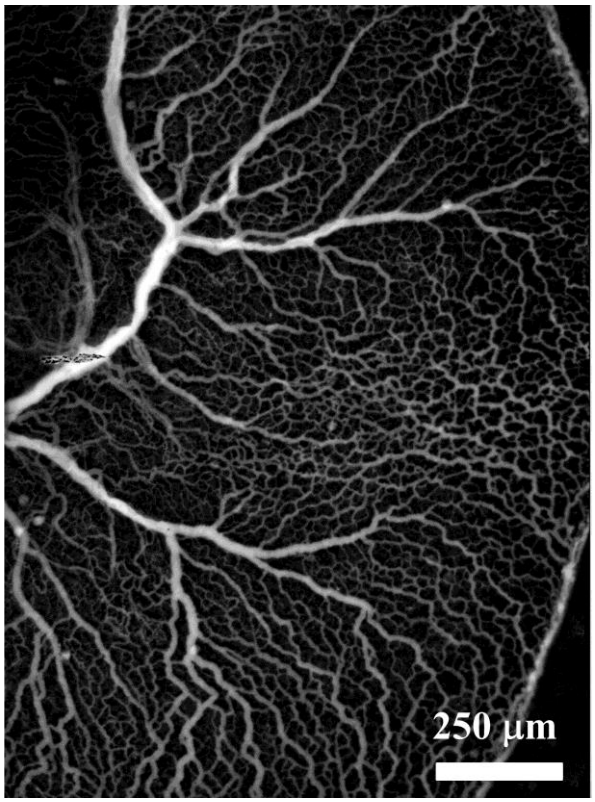
250 μm

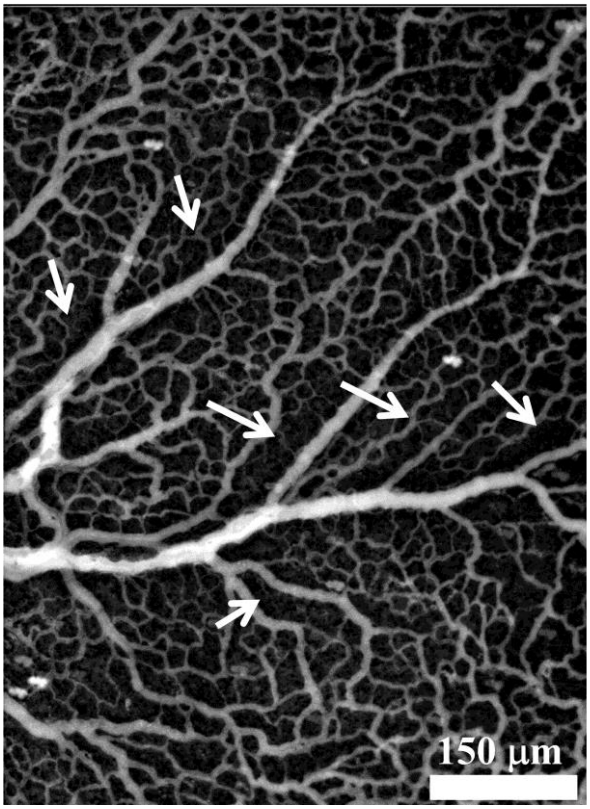
150 μm

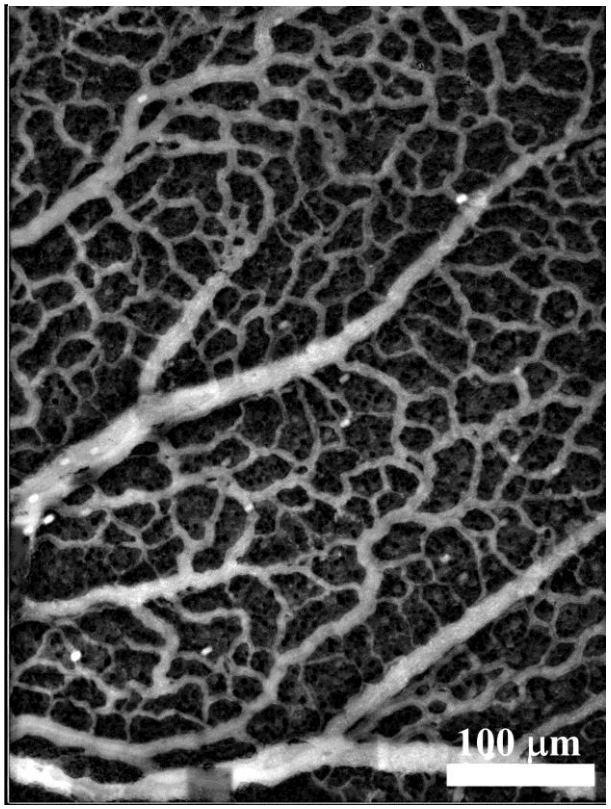
100 μm

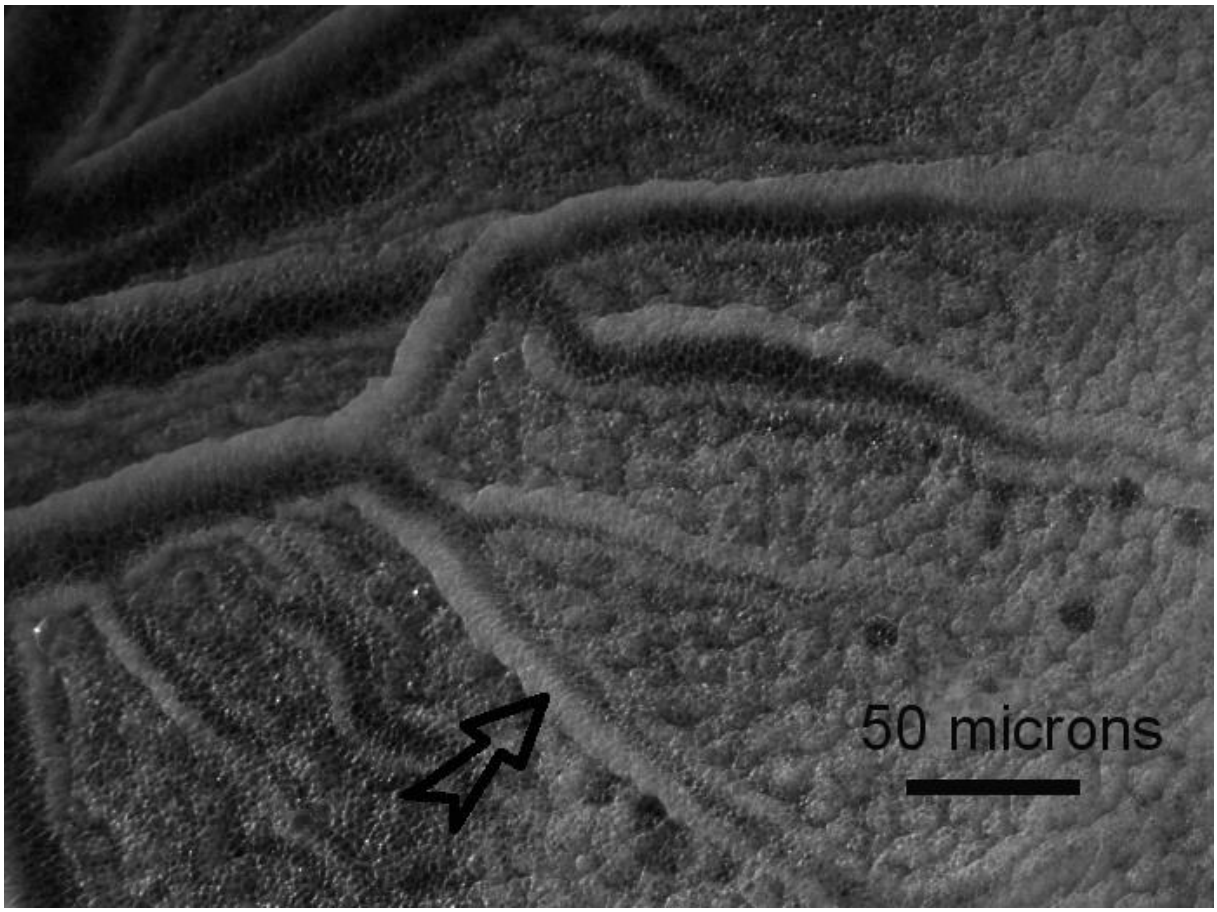
50 microns

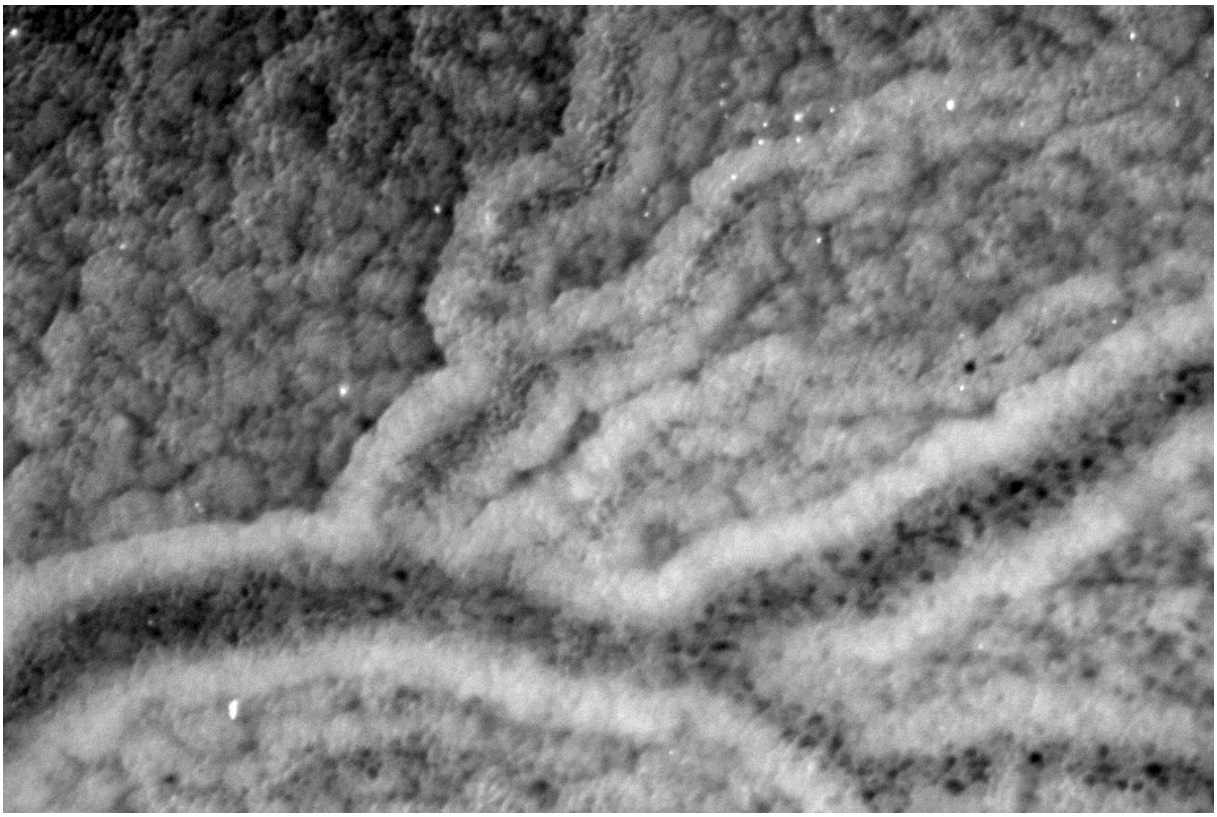

Figure 7D

Figure 7. Localized cell swelling along blood vessels. Fig. 7A Normal blood vessels are imaged in the Yolk Sac both from atop and from underneath and in shadowgraph (which reveals surface volumes). One observes that the normal blood vessels are lined with a swollen neighborhood, which appears whiter because the capillary density is decreased (middle, arrow). The shadowgraph image (Left) shows a swollen area. To the right, the underneath view reveals that the swelling is in the endoderm lining the vessels. Fig. 7B A magnified view of the cells wrapping an arteriole shows large cuboidal swollen cells. Fig. 7C observation of the normal Yolk Sac vasculature shows regions along arterioles in which capillary density is diminished (arrows). Fig. 7D Comparison of the normal endoderm, and the endoderm exposed to an osmotic shock. It is observed that the swollen endoderm normally present along the vessels swells even more up to the point that the swollen areas come to confluence and crush capillaries.

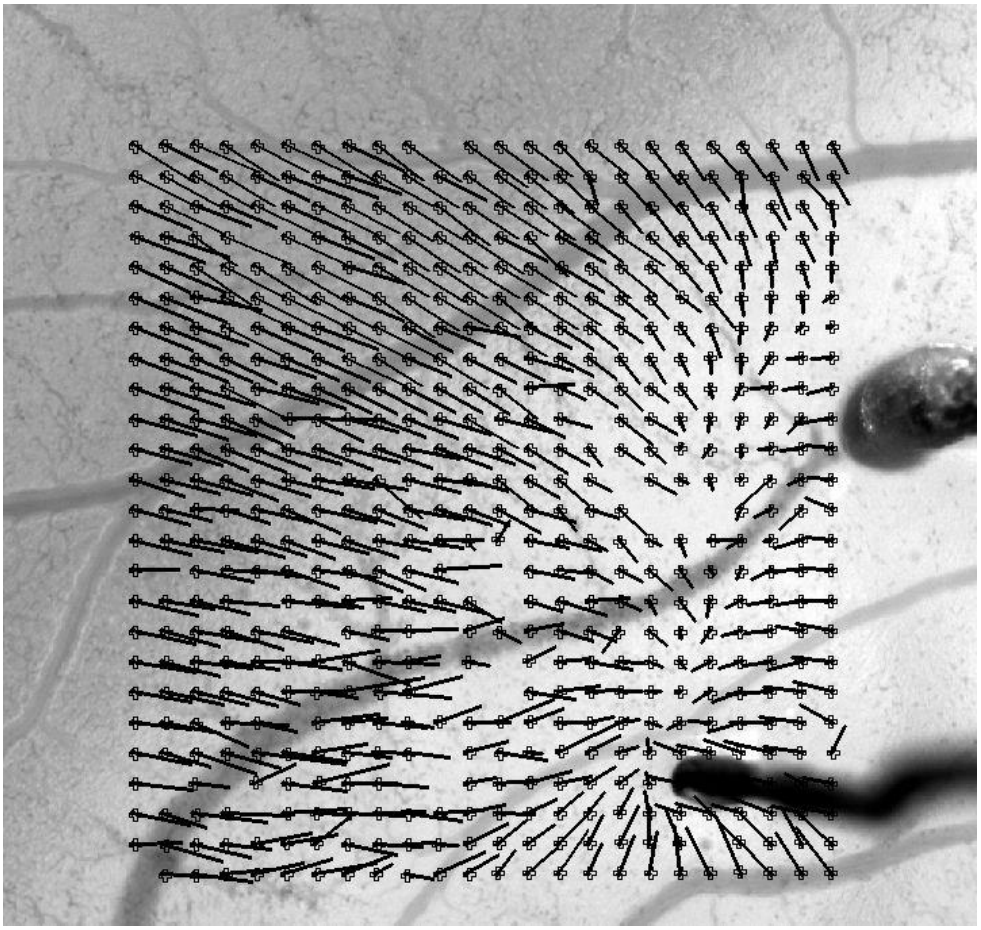

Figure 8A

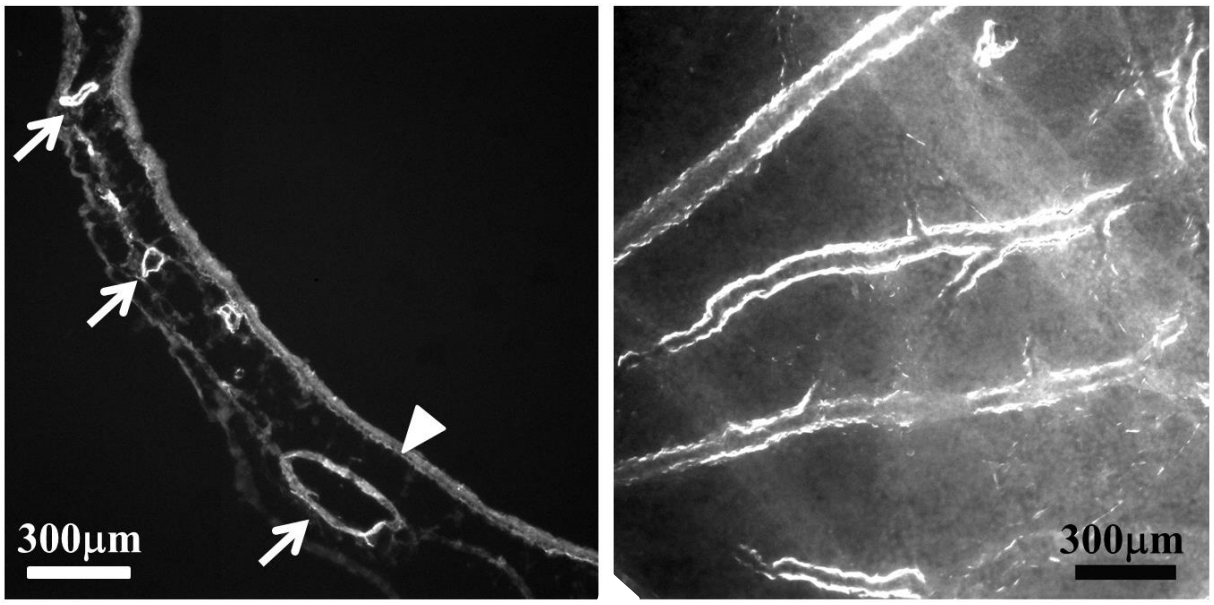

Figure 8B

Figure 8. Contraction under electric shocks. Fig. 8A In order to check that the CAM is intrinsically contractile, we perfomed simple electric shocks, following the experiments presented in Ref. 25. We observed that the CAM responded in 100% of the cases to a small electric shock of duration 5 seconds, and value between 0.1 and 0.5 V by a strong contraction causing a localized ischemia much similar to the one observed in the Mannitol assay (Video 6). The map shows the displacement map between two electrodes, for a 0.1V shock between two electrodes, and a time interval of 15 minutes. The displacements are calculated by PIV, and the straight black bar represents the vector of displacement between the reference configuration, and the deformed configuration (gaps in the data correspond to aberrant displacements where the Tracker Module (PIV software) does not manage to calculate the displacement by correlation function). Fig. 8B We also checked the presence of α-Actin by immuno-staining. Fig. 8B shows staining for α-Actin in CAM sections (Left), and in toto (Right). Both reveal the presence of α-Actin around the vessels (arrow), and in a thin layer in the surface ectoderm of the CAM (arrowhead)

Supplementary Material Figure 1

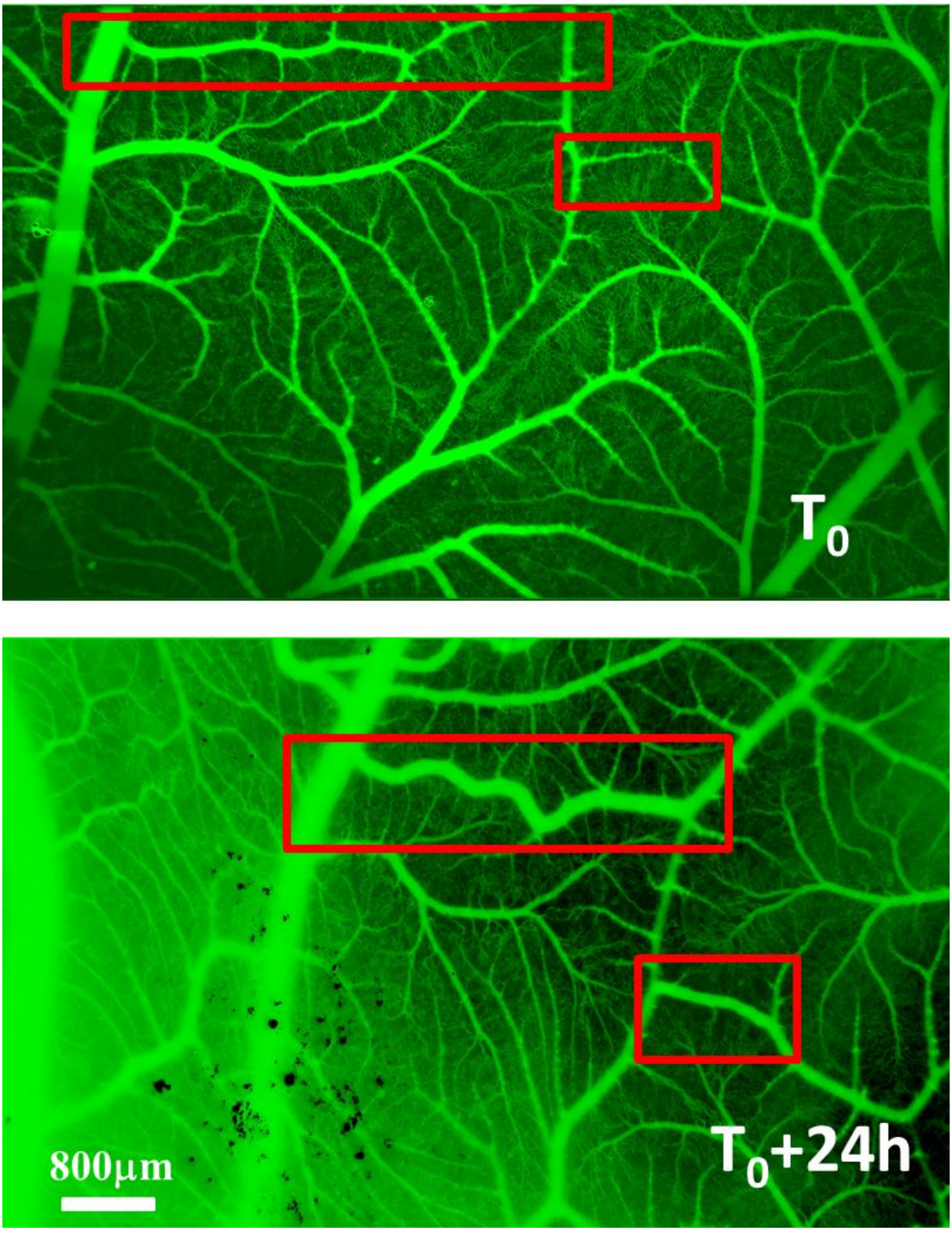

Supplementary Figure 1A

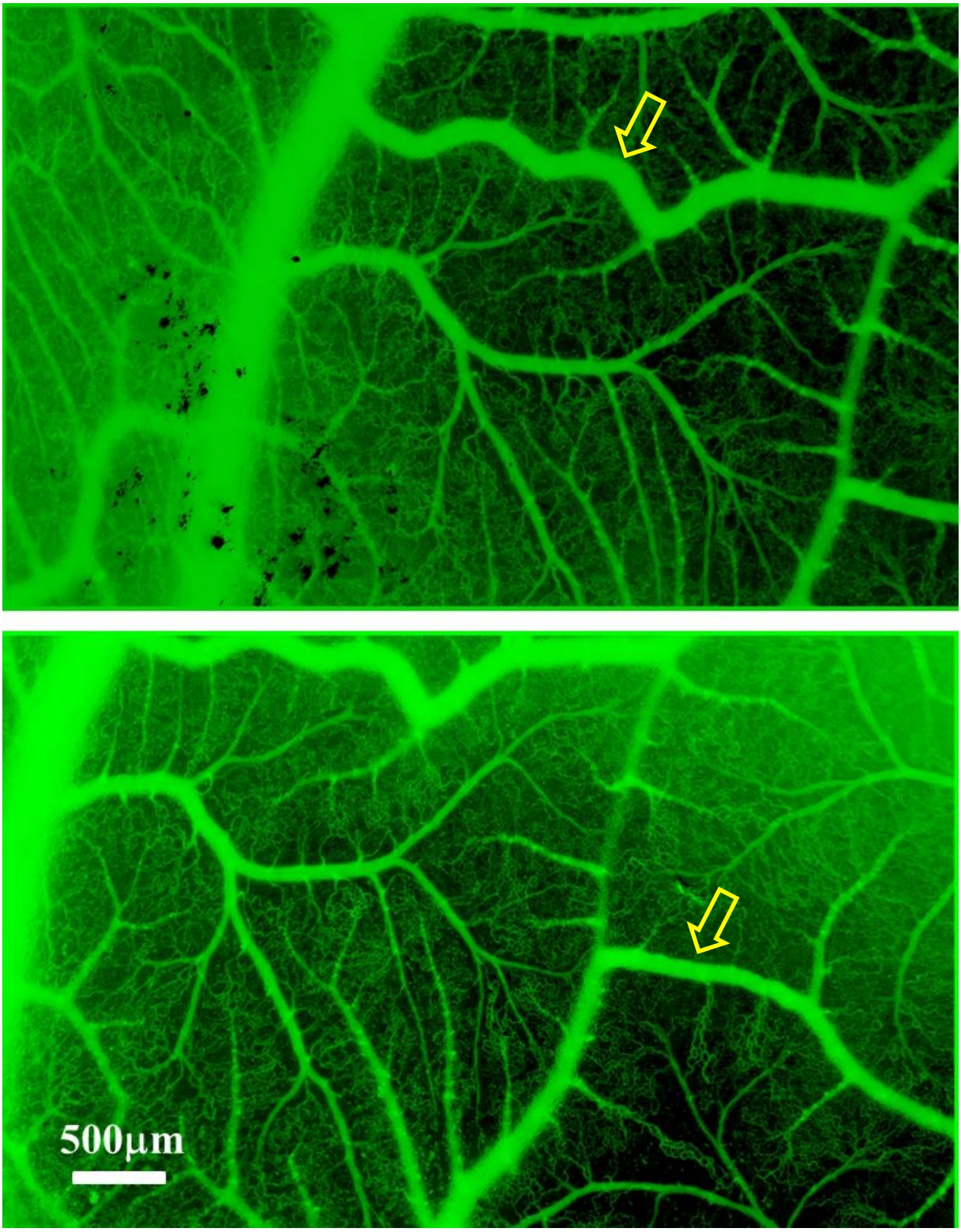

Supplementary Figure 1B

Supplementary Figure 1 Example of aberrant anastomoses formed during exposure to Mannitol 5% (arrows in Supp. Fig. 1B).This is a relatively rare event, observed approx. 10% of the times. This phenomenon is difficult to study systematically, because of statistical rarity, however, it may have a clinical importance. It might be possible that the aberrant mechanical state induced by the Mannitol assay selects areas where the normal situation has created an already statistically limiting configuration (limiting proximity). (Fig. 1A Mag. 1.25X, Fig. 2B Mag. 2X). The varicose aspect of the larger anastomose to the Top is obviously due to longitudinal contraction during the assay (see the shrinkage of the red box).